NASA Technical Memorandum 85847

NASA-TM-85847 19840006028

Origin and Evolution of The Saturn System

James B. Pollack and Guy Consolmagno

November 1983

National Aeronautics and
Space Administration

NASA Technical Memorandum 85847

Origin and Evolution of The Saturn System

James B. Pollack, Ames Research Center, Moffett Field, CA
Guy Consolmagno, Massachusetts Institute of Technology, Cambridge, MA

NASA
National Aeronautics and
Space Administration

Ames Research Center
Moffett Field, California 94035

N84-14096#

Abstract

As was the case for Jupiter, Saturn formed either as a result of a gas instability within the solar nebula or the accretion of a solid core that induced an instability within the surrounding solar nebula. In either case, the proto-planet's history can be divided into three major stages: early, quasi-hydrostatic evolution (stage 1); hydrodynamical collapse (stage 2); and late, quasi-hydrostatic contraction (stage 3). During stage 1, Saturn had a radius of several hundred times that of its present radius, R_s, while stage 3 began when Saturn had a radius of $\sim 3.5\ R_s$. Stages 1 and 2 lasted $\sim 10^6$-10^7 years and ~1 year, respectively, while stage 3 is continuing through the present epoch.

Saturn's current excess luminosity is due, in part, to the loss of thermal energy built up by a faster contraction that marked the earliest phases of stage 3. But, in contrast to the situation for Jupiter, this internal energy source fails by a factor of several in producing the observed excess luminosity. The remainder is most likely due to the gravitational separation of helium from hydrogen due to its partial immiscibility in the outer region of the metallic hydrogen zone.

The irregular satellite Phoebe was most likely captured by gas drag experienced in its passage through a bloated Saturn, just prior to the onset of stage 2. During stage 2, a nebular disk formed from the outermost portions of Saturn, due to a progressive increase in their rotational velocity as the planet contracted. This increase may have been enhanced significantly by a transfer of angular momentum from the inner to the outer regions of the planet. The nebular disk served as the birthplace of Saturn's regular satellites and probably the ring material. Viscous dissipation within the nebula caused an inward transfer of mass, and thus

may have determined the nebula's lifetime, and an outward transfer of angular momentum. It is not clear what the relative roles of Saturn's luminosity and viscous dissipation were in determining the nebula's radial temperature structure and its evolution with time.

As Saturn's excess luminosity declined or less viscous dissipation in the nebula occurred during the early portion of stage 3, water was able to condense at progressively closer distances to the center of the system and water clathrates and hydrates were able to form throughout much of the nebula, especially in its outer regions. It is the likely presence of ices other than pure water ice in at least some of the regular moons of Saturn that make them chemically distinct from the large icy moons of Jupiter. If Saturn's nebula had a high enough pressure (greater than several tens of bars) in its inner region, a liquid solution of water and ammonia, rather than water ice, would have been the first "icy" condensate to form.

Despite the comparatively small size (hundreds to about a thousand kilometers) of the inner moons of Saturn, a number, especially Dione and Rhea, may have experienced significant expansion and melting during the first $\sim 1 \times 10^9$ years due to the presence of substantial quantities of ammonia monohydrate (~10-20% by weight). The occurrence of the youngest known surfaces in the Saturn system on the comparatively small sized Enceladus is most readily attributed to strong tidal heating created by its forced orbital eccentricity. But a significantly larger eccentricity is required at some time in its past for tidal heating to be quantitatively capable of initiating melting, with the current eccentricity being perhaps large enough to maintain a molten interior.

During the early history of the Saturn system, giant impact events may have catastrophically disrupted most of the original satellites of Saturn. Such disruption, followed by reaccretion, may be responsible, in part, for the occurrence of "Trojans" and "co-orbital" moons in the Saturn system, the apparent presence of a stochastic component in the trend of satellite density with radial distance, and the present population of ring particles.

Titan's atmosphere formed from the hydrates and clathrates — especially ammonia monohydrate and/or nitrogen clathrate and methane clathrate — that constituted the satellite. Over the age of the solar system, a nontrivial amount of atmospheric nitrogen (about several tens of percent of the current atmospheric inventory) and much more methane than is presently in the atmosphere have been lost, through a combination of N and H escape to space and the irreversible formation of organic compounds. These considerations imply quasi-real time buffering of atmospheric methane by a near-surface methane reservoir and the existence of a layer of 0.1-1 km thickness of organic compounds close to or on Titan's surface.

I. Introduction

The Saturn system resembles the Jupiter system in a number of ways. The planet Saturn is massive (~95 Earth masses) by the standards of the inner solar system and is composed chiefly of hydrogen and helium. However, like Jupiter, it has a central core of "rock" (silicate and iron compounds) and perhaps "ice."[a] The planet has an internal heat source that causes it to radiate to space about twice as much energy as the amount of sunlight it absorbs. Surrounding Saturn is a miniature solar system composed of at least 16 "regular" satellites, one captured satellite (Phoebe), and, of course, its magnificent set of rings.

In all the above regards, the Saturn system differs markedly from the planets of the inner solar system. The terrestrial planets are much less massive; they are made almost entirely of "rock"; their internal heat source is orders of magnitude smaller than the amount of sunlight they absorb; and there are only three satellites, with perhaps all of them (or at least Phobos and Deimos) being captured objects.

Upon closer examination, however, the Saturn system differs in a number of important ways from the Jupiter system. First, Saturn's central core represents a larger fraction of the planet's mass, although the two core masses are quite similar in absolute value. Second (as discussed below) precipitation of helium may provide the chief energy source for Saturn's internal heat flux, whereas thermal cooling may act as the chief

---

[a]By "ice," we mean compounds derived from low temperature condensates, such as water ice, ammonia hydrate, and methane clathrate. Naturally, at the conditions of Jupiter's interior, an "ice" component would be a supercritical fluid.

energy source for Jupiter. Water ice appears to be a major constituent of all of Saturn's regular satellites, whereas it is at best a minor component of Jupiter's innermost satellites. The Jupiter system has two families of irregular satellites, but the Saturn system has only one known irregular satellite. Finally, Saturn's rings are much more prominent and much more massive than that of Jupiter.

In this chapter, we review our current understanding of the origin and evolution of the Saturn system and its individual components. We will seek not only to view Saturn in isolation, but also to compare theories of its history with those for Jupiter, the other giant planets, and the terrestrial planets. In so doing, we will attempt to understand the similarities and differences among these objects, as noted above, and to test the internal self-consistency of alternative theories.

II. Critical Constraints

Certain key observational data on the Saturn system are relevant to understanding its history. Some of these constraints were derived from Earth-based observations. However, measurements conducted from the Pioneer 11 and Voyager 1 and 2 spacecraft have greatly supplemented these results.

Models of Saturn's interior, constrained to match the planet's mass, radius, and J_2 and J_4 gravitational moments, suggest that it consists of two major, compositionally distinct zones: a central core with a mass of 20 ±5 $M_\oplus$ (earth masses) made of an unknown mixture of "rock" and "ice"; and an outer fluid envelope with a mass of 75 ±5 $M_\oplus$ made of an approximately solar mixture of elements (Slattery, 1977; Podolak, 1978; Hubbard and MacFarlane, 1979; Grossman et al., 1980; Stevenson, 1982). This value for the core mass lies within a factor of two of the core masses of Jupiter, Uranus, and Neptune, despite a factor of 20 variance in their total masses.

The hydrogen-helium dominated envelope consists of two major regions that are distinguished by the phase of hydrogen in them. At pressures less than a few megabars, hydrogen is present as molecular hydrogen, H_2, a good electrical insulator, while at higher pressures it occurs as metallic hydrogen, a good conductor. Saturn's metallic H zone constitutes about 20% of its envelope's mass, in contrast to a value of about 70% for Jupiter.

There are several tentative deviations of the composition of Saturn's observable atmosphere from that expected for a solar mixture of elements. First, the helium mass fraction, Y, in Saturn's atmosphere appears to be significantly smaller than the corresponding value for Jupiter — 0.11 ±0.03 versus 0.19 ±0.05 (Hanel et al., 1981). The latter value is close to the solar value. If true, this difference could be due to a preferential segregation of He toward the bottom of Saturn's envelope, driven by the partial immiscibility of He in metallic H at low temperatures (Salpeter, 1973; Stevenson and Salpeter, 1977). Note, however, that the calculation of the conditions under which immiscibility commences is very difficult and one recent calculation would rule out such an effect for the temperature and pressure conditions characteristic of Saturn's metallic H zone (MacFarlane and Hubbard, 1983). Other deviations from solar elemental ratios may include an approximately twofold enhancement of the C/H ratio in Saturn's atmosphere.

Saturn radiates to space about 1.79 ±0.10 times as much energy as the amount of sunlight it absorbs (Hanel et al., 1982). The implied excess luminosity, due to an internal heat source, is about four times smaller than Jupiter's excess luminosity, is about 1 1/2 orders of magnitude greater than Neptune's, and is at least 1 1/2 orders of magnitude greater than Uranus' as yet undetected excess (Stevenson, 1982).

The rings of Saturn are composed of a myriad of particles in independent orbits about the planet. The principal rings — A, B, and C — are located between 1.21 and 2.26 R_s from the center of Saturn, where R_s is the planet's equatorial radius. Thus, these rings lie within the classical Roche tidal radius, as do the rings of Jupiter and Uranus. However, fainter rings of the Saturn system are located both closer to the planet and farther away, including distances outside the Roche limit (see Table 3 of Stone and Miner, 1981).

Most of the particles in the main rings have radii that lie between 0.1 cm and a few meters (Pollack et al., 1973; Cuzzi and Pollack, 1978; Cuzzi et al., 1980; Tyler et al., 1981). Much smaller, micron sized particles are present in some portions of the rings, such as the F ring and the spokes of the B ring (Pollack, 1981; Smith et al., 1981). The latter particles have lifetimes that are probably much less than the age of the solar system, due to catastrophic impacts with micrometeoroids, and are thus most likely the products of the continued erosion of the larger ring particles by micrometeoroid impact (Pollack, 1981). Water ice is the dominant material that makes up both the surfaces and interiors of the centimeter to meter sized ring particles (Pilcher et al., 1970; Pollack, 1973; Cuzzi et al., 1980). Although "rock" may be present as a minor coloring agent (Lebofsky et al., 1970), an upper limit on its bulk abundance appears to lie far below that expected from solar abundance considerations (Pollack et al., 1973; Cuzzi et al., 1980). Finally, the rings have a mass of about 6.4×10^{-8} Saturn masses, a value comparable to that of the satellite Mimas (Holberg et al., 1982).

The Saturn system contains 17 known satellites, whose locations range from just outside the A ring (1980 S28) at 2.28 R_s to 215 R_s (Phoebe) and whose sizes range from a diameter of 30 km (1980 S28) to 5150 km (Titan) (see Table 1). All the satellites but Phoebe travel in prograde orbits having low eccentricities and low inclinations to Saturn's equatorial plane (Iapetus' inclination of 15° may be due to the Sun's tidal torque on Saturn's protosatellite nebula (Ward, 1981). Such a torque significantly warped the plane of the nebula toward the LaPlacian plane at great distances from the planet). Thus all the "regular" satellites were presumably formed coevally and from the same cloud that gave birth to Saturn, while Phoebe is most likely a captured object.

As summarized in Table 1 and Figure 1, all the regular satellites whose mean densities have been measured have densities below 2 g/cm^3. The corresponding uncompressed mean densities fall well below those of the inner Galilean satellites of Jupiter and well below those characterizing unhydrated (>3 g/cm^3) and hydrated (≥2.3 g/cm^3) rock. Thus, "ice" (mostly water) represents a major component of their interiors, in addition to "rock." On the <u>average</u>, the uncompressed mean density of the Saturnian satellites is comparable to that expected for a solar abundance of ice and rock (about equal masses) and similar to those of the outer Galilean satellites. There is no obvious trend in the mean densities as a function of distance from Saturn, in contrast to the situation for the Galilean satellites. Furthermore, there may be significant, but stochastic, departures of individual values from their mean value.

Water ice is also a major constituent of the surfaces of the regular satellites. This conclusion is based on the presence of water ice absorption features in the near infrared reflectivity spectra of the larger satellites (Cr kshank et al., 1979; Fink et al., 1976) and the high albedo in the visible f all the regular satellites but Titan (whose surface is masked by an o ically thick smog layer) and the leading side of Iapetus (see Table 1). In the case of the smaller and presumably undifferentiated satellites, a ter rich surface implies a water rich interior.

The very w albedo of Phoebe and the shape of its visible and near infrared refle ivity spectrum imply that it is made of carbonaceous chondritic-lik material (Degewij et al., 1980). Its reflectivity spectrum closely matche those of Jupiter's irregular satellites, all studied Trojan asteroids, and C" type objects in the main asteroid belt.

The geolo cal histories of all the Saturnian satellites have been strongly influe ced by meteoroid impact events, while tectonism and resurfacing events ve also played important roles for the larger satellites (Smith et al., 981 and 1982). The high crater density on parts or all of the surfaces o almost all the Saturnian satellites has commonly been interpreted, b lunar analogy, as reflecting an early period (first $\sim 1 \times 10^9$ years) of heavy meteoroid bombardment. Furthermore, there is substantial ev ence implying that some of the original satellites were catastrophical disrupted during this period: Several objects have almost identical orbit , including the small co-orbital satellites 1980 S1 and S3, Tethys and its rojans (1980 S13 and S25), and Dione and its Trojan (1980 S6); obj ts as big as Hyperion have distinctly nonspherical shapes; and extrapolat n of the crater density on Iapetus to the inner parts of the Saturn syst m, with an allowance for gravitational focusing, results in a near-unit robability of catastrophic disruption of the smaller, innermost satellite

Several of the larger satellites, including Tethys, Dione, and Rhea, have global scale fractures of their surfaces, indicative of extensional tectonism. The relatively low crater densities on this portion of their surfaces imply that tectonism extended to the end of or beyond the epoch of heavy bombardment. There are also surface morphologies on these bodies indicative of resurfacing events in the late or post heavy bombardment epoch. Perhaps most surprisingly of all, the comparatively small satellite Enceladus has a very low crater density over much of its surface, exhibits grooves somewhat reminiscent of those on Ganymede, and has experienced extensive resurfacing. On the basis of crater densities, these extensional tectonic and resurfacing events have extended up until relatively recent times (within the last $\sim 1 \times 10^9$ years). Finally, there is the classical puzzle of at least an order of magnitude variation in the brightness of Iapetus from the dark leading hemisphere to the bright trailing hemisphere.

Titan is the only satellite known to have a substantial atmosphere. Measurements made from the Voyager 1 spacecraft yielded a surface pressure of 1.6 bars (Tyler et al., 1981), with molecular nitrogen being the dominant gas (Tyler et al., 1981; Samuelson et al., 1981). The volume mixing ratio of N_2 lies between 80% and 95%. Other major constituents include methane (few percent) and molecular hydrogen (0.2%). There is also indirect evidence for the possible presence of substantial quantities of Ar (~10%) based on the value of the mean molecular weight, derived from comparing radio occultation and IRIS temperature profiles (Samuelson et al., 1981). Trace gases that are present at the ppm level include low order hydrocarbons, such as C_2H_2 and C_2H_6, and nitrogen containing organics such as HCN (Hanel et al., 1981). One very recent surprise has been the detection of oxidized gases at the ppb (CO_2) and ppm (CO) levels (Samuelson et al., 1983; Lutz et al., 1983). Finally, a pervasive smog layer is present throughout the lowest several hundred kilometers of the atmosphere (Smith et al., 1981 and 1982). The smog particles are probably made of complex organic polymers that are end products of the photochemistry occurring in Titan's atmosphere.

III. Formation and Evolution of Saturn

a. Origin

As discussed in Section II, Saturn consists of a 20 $M_\oplus$ core made of rock and ice and a 75 $M_\oplus$ envelope containing approximately a solar mixture of elements. Such a structure suggests two alternative theories for the origin of the Saturn system: either a gaseous condensation first formed within the solar nebula and it later acquired core material (gas instability theory) or solid body accretion occurred first, with the core mass eventually becoming large enough to effectively concentrate an even greater mass of solar nebula gas about itself (core instability theory). During the last 10 years, both theories have been studied in some detail.

According to the gas instability theory, the solar nebula was sufficiently massive ($\gtrsim 0.1\ M_\oplus$) that it was unstable to global, azimuthal perturbations (Cameron, 1978) (see Fig. 2). As a result of this gravitational instability, rings of elevated density formed and grew progressively narrower. Eventually, the gas density within the ring became high enough for local gravitational instabilities to occur. The resultant giant gas balls within a given ring may have either merged with one another or gravitationally deflected one another to different orbits. The resultant giant gaseous protoplanets subsequently gravitationally contracted to form the outer planets.

The above scenario, according to which giant gaseous protoplanets form from a series of instabilities in a massive solar nebula, is far from proven.

For example, spiral density waves rather than ring instabilities may be the fastest growing mode in an unstable massive nebula (P. Cassen, private communication).

There are two ways in which the giant gaseous protoplanets may have acquired their cores. First, as they contracted and grew hotter, pressure and temperature conditions within their deep interior may have permitted solid grains to become liquid grains, and subsequently coalesce efficiently into large sized particles. Such particles would have large terminal velocities and tend to precipitate to the protoplanet's center to form a core (Slattery et al., 1980). This mechanism is important for Saturn's core only if there is a large exchange of material between the solar nebula and the protoplanet: Saturn's core represents about 20% of the planet's mass, whereas heavy elements constitute only about 1% of the mass in a solar mixture of elements. Furthermore, standard interior models require an excess of heavy elements in the core rather than a mere redistribution of elements. Thus, one must postulate a continual replenishment of refractory materials from the nearby solar nebula so that a 20 $M_{\oplus}$ core can be constructed.

Only the more refractory materials become liquid inside protoplanets and so contribute to the cores, according to the calculations of Slattery et al. (1980). But solids can also coagulate, although somewhat less efficiently than liquids, so that it is not clear that the grains need to go through a liquid phase to sink to the protoplanet's center. In any case, it seems unlikely that cores containing ices could be formed through this mechanism in view of the high temperatures in the deep interior of the protoplanets during almost all of their lifetime.

A second mechanism by which giant gaseous protoplanets could acquire cores is through gas drag capture of solid planetesimals that formed nearby in the solar nebula (Pollack et al., 1977). In the next section, it will be argued that this mechanism is the most likely means by which Phoebe was captured. However, an irregular satellite rather than core material is the end product of gas drag capture only for a very short time interval (~10 years) in the history of the protoplanet and only for bodies lying within a restricted mass range. Thus, if Phoebe was captured by gas drag, many orders of magnitude more mass would have been contributed to the core by other captured planetesimals. Whether as much as a 20 $M_\oplus$ core could have been acquired in this manner is open to question. To the degree that Phoebe is representative of the planetesimals present near Saturn during its very early history, we would expect that core material resulting from gas drag capture would be lacking significant amounts of nitrogen compounds and would have an excess of rock over water and carbon compounds. Thus, neither core formation mechanism is expected to lead to significant quantities of nitrogen compounds in the core and only limited amounts of water and carbon compounds at best.

According to the alternative "core instability" model (Perri and Cameron, 1974; Hayashi et al., 1977; Mizuno, 1980), accretional processes involving solid planetesimals led to the growth of planet-sized objects in the outer solar system as well as in the inner solar system. As the solid cores grew larger, they concentrated solar nebula gas more and more effectively within their tidal sphere of influence. Eventually, the envelopes became sufficiently massive that they became gravitationally unstable and underwent a hydrodynamical collapse onto the central core. Such a collapse insures the ultimate survival of the envelope against tidal disruption by the forming Sun; leads to a compact object; and can result in a further significant increase in the mass of the envelope as additional material from the solar nebula enters within the object's gravitational sphere of influence.

Estimates of the core mass at which instability first occurs have been obtained by constructing static equilibrium models of core/envelope configurations and determining the largest core mass for which such a model can be constructed. The first models of this type were constructed by Cameron and Perri (1974), who assumed that the temperature structure was adiabatic throughout the envelope. They obtained "critical" core masses of about 70 $M_{\oplus}$ for Saturn, with the value of the critical core mass being somewhat sensitive to the boundary conditions and thus position within the solar nebula. Both the large value of the critical mass and its sensitivity to position resulted in a poor match with the inferred core masses of Saturn and the other giant planets.

Both problems have been overcome in more recent models, in which the temperature structure has been calculated rather than assumed. The occurrence of a zone of radiative equilibrium in the outer portion of the envelope results in both a lower critical core mass and an insensitivity of this mass to boundary conditions (Mizuno, 1980). Throughout all but the hot inner parts of the envelope, the radiative opacity is dominated by grains, whose properties therefore determine the temperature structure of the envelope. Figure 3 illustrates the relationship between core mass and total mass, where the parameter f denotes the ratio of the actual grain opacity to that expected from grains in a cool solar nebula. For each choice of f, there is a maximum value of core mass ("critical value"). It is not possible to find a static equilibrium configuration for core masses exceeding this critical value. As can be seen, this value does not depend sensitively on f. Critical core masses comparable to that of Saturn are obtained for models having $f \sim 1$.

Unfortunately, these models of Mizuno and more generally the earlier ones as well suffer from several potentially serious problems. First, the inability to construct a hydrostatic model for large core masses is not equivalent to such models undergoing hydrodynamic collapse. These models could, in principle, undergo a slow contraction or expansion and indeed such behavior would be expected in general for accretionary objects radiating to space. In a similar vein, no fundamental physical change in the interior of these models is cited to suggest that hydrodynamic collapse should occur for the large core models. Second, it is not clear that the tidal radius is the appropriate outer boundary of these primordial planets, as assumed in all the above calculations. An alternative choice is the accretionary radius, where the thermal energy of the gas balances in absolute magnitude its gravitational energy. Certainly for small enough core masses, the accretionary radius is smaller than the tidal radius and is, therefore, the more appropriate choice. Consequently, there may be more sensitivity to boundary conditions than when only the tidal radius is considered.

Very recently, Bodenheimer and Pollack (1983) have carried out a series of calculations of the accretionary growth of core models that overcome the above problems. They find that when the core mass grows sufficiently large a hydrodynamic collapse does in fact occur, due to the occurrence of high enough temperatures for molecular hydrogen to dissociate in a significant portion of the deep interior of the envelope. Critical core masses of about 10 $M_\oplus$ characterize their models at the point of collapse, but with this mass varying by factors of several depending on the assumed nebular boundary conditions and core accretion rate. Much larger variances were found for the envelope mass at the point of collapse, with the envelope mass varying from a small to a large fraction of the core mass. In contrast, Mizuno's (1980) calculations indicated that the envelope mass was always a significant fraction (~0.7) of the critical core mass.

Once hydrodynamic collapse occurs, gases may be added much more rapidly to the protoplanet than planetesimals to the core. Thus, the envelope mass may grow much more rapidly after collapse than does the core mass. Preliminary studies of this and the earlier phases have been conducted by Safronov and Ruskol (1982). They distinguish six stages of formation and growth. Stage 1 is equivalent to the accretional growth of the core and ends with it reaching the critical core mass. Since the core as well as the envelope can grow somewhat during the subsequent stages, the critical core mass is assumed to be a few $M_\oplus$ rather than 20 $M_\oplus$. During stage 2, accretion of gas from the solar nebula is limited by the time required to radiate away part of the gravitational energy of accretion so that thermal pressure does not prevent the added mass from lying within the protoplanet's sphere of influence. During stage 3, an unrestricted rapid growth occurs. During stage 4, accretion is limited by the size of the sphere of influence. During stages 5 and 6 accretion is further limited by the need to resupply gas from distant parts of the solar nebula to parts lying close to the protoplanet's orbit and by the dissipation of the solar nebula, respectively. Estimates of the duration and amount of mass added to Jupiter and Saturn during each stage are summarized in Table 2. According to these estimates, several times 10^8 years are required before Saturn's growth is completed. A slightly smaller time scale is found for Jupiter.

Both of the above models – core and gas instability – have their strong and weak points. If only the outer planets formed as a result of gas instabilities in the solar nebula, it seems likely that Jupiter might have formed before much accretional growth of solid bodies took place in the inner solar system. In this event, Jupiter could have interfered with the accretional growth of solid bodies within the asteroid belt and in the vicinity of Mars' orbit, by gravitationally perturbing orbits of nearby planetesimals into ones that crossed those of the more distant asteroidal and Martian planetesimals at high relative velocities. In this way, the absence of a single planet-sized body in the asteroid belt and the relatively small size of Mars could be accounted for. However, if gaseous protoplanets formed throughout the solar nebula, as has been proposed by Cameron (1978), then the ability of this theory to explain the size of Mars and the multiplicity of asteroids is less clear. If the terrestrial planets initially had massive gaseous envelopes, their envelopes could have been eliminated by the tidal action of the forming Sun (Cameron, 1978) or thermal evaporation as the solar nebula heated up (Cameron et al., 1982). Because of their greater distance from the Sun, the outer planets were less susceptible to tidal stripping and thermal evaporation.

The gas instability model has a number of serious problems. First, it does not provide an obvious explanation for the similarity of the core masses of the four giant planets. Second, if the inner planets also formed as a result of gas instabilities and if they acquired their cores by precipitation of liquids or solids in their envelopes, then it is not clear why the uncompressed densities of the terrestrial planets tend to decrease from Mercury to Mars or why the abundance of primordial rare gases systematically increases by orders of magnitude from Mars to Venus. Finally, it remains to be demonstrated that the large enrichment of heavy elements in the giant planets can be achieved through a combination of precipitation and gas drag capture. This problem may be especially serious for Uranus and Neptune, whose cores constitute 80-90% of the planets' total mass.

We next assess the viability of the core instability model. As explained above, the critical core mass required to induce an instability in the surrounding solar nebula is somewhat insensitive to the boundary conditions at the tidal radius and hence to pressure and temperature conditions within the solar nebula. In this sense, it provides a natural explanation for the similarity of the core masses of the giant planets. Second, a much larger variance is expected in the masses of the envelopes, as in fact is observed, due to the large variance in these masses at the point of collapse and the subsequent preferential accretionary growth of the envelope after collapse. Also note that the calculations of Bodenheimer and Pollack (1983), unlike those of Mizuno (1980), permit the masses of the envelopes of Uranus and Neptune to be a minor fraction (10-20%) of the planets' total mass. Third, it seems likely that the smaller bodies of the solar system — asteroids, comets, and satellites — formed by accretional growth. On aesthetic grounds, it might seem preferable for this same process to account for the mean density (Lewis, 1972) and for the rare gas content of the terrestrial planets (Wetherill, 1981; Pollack and Black, 1979 and 1982) as well as the formation of the giant planets.

However, the core instability theory also has problems. In particular, there are problems connected with time scales. Because Jupiter's core probably formed in a region of the solar nebula of lower density than did Mars or the asteroid belt, and because its core mass is much greater than even the mass of the Earth, Jupiter should have formed after Mars and the asteroid parent bodies did. In this event, Jupiter could not have interfered with their growth.

Also, the time scales for core growth progressively increase with distance from the center of the solar nebula due to a combination of the lower volume densities and longer orbital periods of planetesimals at greater distances. This time scale approaches the age of the solar system for Uranus and Neptune and therefore apparently exceeds the lifetime of the solar nebula for these planets (Safronov and Ruskol, 1982). However, this estimate of the time scale for core growth is based on a theory of planetesimal assembly in a gas-free environment, surely an invalid assumption for the giant planet models under discussion. Gas drag might significantly expedite core growth.

Finally, to some extent, the two origin theories can be distinguished on the basis of the mass of the solar nebula they imply. A nebular mass in excess of about 0.1 $M_{\odot}$ is required for gas instabilities to occur with a 1 solar mass sun at the nebula's center, whereas nebular masses ranging from 0.01 $M_{\odot}$ to 0.1 $M_{\odot}$ are typically invoked in models having solid accretional growth. The expected mass of the solar nebula is related to the angular momentum of the cloud from which the solar system formed (Cameron, 1978). While Cameron (1978) advances astrophysical arguments in favor of a large angular momentum and hence a large nebula mass, almost all of the angular momentum must be lost to match the current angular momentum of the solar system. It seems difficult to discriminate between these two theories on the basis of the implied nebular mass or cloud angular momentum in view of the poor independent constraints on either of these quantities.

b. Evolution

According to both theories of its formation, Saturn underwent three major phases in its evolution during and following formation: early quasi-hydrostatic contraction or expansion (stage 1), hydrodynamical collapse (stage 2), and late, quasi-hydrostatic contraction (stage 3). During stage 1, the envelope was in hydrostatic equilibrium to a very good first approximation. In the case of the gas instability model, the envelope slowly contracted from about 1600 R_s to about 60 R_s on a time scale of 4.6×10^6 years (Bodenheimer et al., 1980). The initial radius is set by Saturn's mass and the minimum density at which a local instability occurs for a solar nebula in which most of the Sun's mass was not yet concentrated near the center of the nebula. The initial radius would be a factor of 8 smaller if the Sun had already fully formed prior to the gas instability.

The time scale for this stage is set by the rate at which the protoplanet radiates to space part of the gravitational energy released by contraction, i.e., it is a Kelvin-Helmholtz time scale. This time scale can be altered by a factor of several by the outer boundary conditions imposed by the solar nebula and by the growth of the Sun at the center of the nebula (Cameron et al., 1981). On the one hand, a non-zero pressure at the boundary results in a faster contraction, while a non-zero temperature has the opposite effect. Since the time scale for stage 1 is comparable to the time scale over which the solar nebula evolves significantly, there is even the possibility that the protoplanet may be tidally disrupted by the forming Sun before it contracts to a small enough radius.

In the case of the core instability model, both the core mass and the envelope mass increase with time during stage 1 (see Fig. 3). The outer boundary of the envelope is a tidal disruption limit, determined by the combined gravitational effects of the solar nebula and the Sun. As the mass of Saturn M increases during stage 1, the outer boundary expands as $M^{1/3}$. The duration of stage 1, in this case, is the accretional time scale required for the core mass to reach its critical value. According to Safronov and Ruskol (1982), stage 1 lasts about 10^8 years for Saturn.

At the end of stage 1, it is no longer possible for pressure gradient forces within the envelope to balance gravitational forces and a hydrodynamical collapse is initiated marking the start of stage 2. From this point on, the planet follows essentially the same evolutionary pathway for both models. The collapse is initiated when the temperatures near the base of the envelope become high enough (~2500 K) for molecular hydrogen to dissociate (Bodenheimer et al., 1980). Stage 2 lasts for only about 0.1 year for Saturn, with this duration being comparable to a free fall time. Collapse first ceases near the center of Saturn due to an increasing stiffness (incompressibility) of the equation of state. Soon, the infalling, outer lying material attains supersonic velocities at the boundary with the static central material, and a shock wave develops (Bodenheimer et al., 1980). Infalling continues until hydrostatic equilibrium has been attained again throughout the entire planet. According to Bodenheimer et al. (1980), Saturn's radius was about 3.4 R_S at the end of stage 2, or almost 20 times smaller than the value at the start of this stage, and the density at the base of envelope increased by almost four orders of magnitude to a value of ~1/3 g/cm^3.

Figure 4 summarizes the time history of Saturn during stages 1 and 2, according to Bodenheimer et al. (1980). For stage 1, these results pertain to a gas instability origin. Also, zero pressure at the exterior boundary and spherical symmetry are assumed. A somewhat different equatorial radius at the start of stage 2 characterizes models in which the rotation and angular momentum of the protoplanet are taken into account (Bodenheimer et al., 1977).

A nebula disk within which the regular satellites and perhaps the rings formed may have come into existence during stage 2, on the basis of the current dimensions of the ring/satellite system. This disk remained attached to the planet, but continued to extend into the region later occupied by satellites due to its initially large specific angular momentum and the outward transfer of angular momentum by viscous dissipation. Because Titan's specific angular momentum is about two orders of magnitude larger than that of Saturn, enough angular momentum redistribution within the protoplanet had to occur during stage 1 and during stage 3 to concentrate the angular momentum in the outermost parts of the system. (Note: Titan dominates the mass of the Saturn ring-satellite system.) Such a redistribution could have occurred by viscous processes, since much of the protoplanet was in convective equilibrium during stage 1, which, in turn, was caused by the high infrared opacity of grains mixed with the gas of the envelope (Bodenheimer et al., 1980). Essentially no angular momentum transport occurred during the very short duration of stage 2, but creation of the nebula disk during this stage was fostered by the decreasing radius of the protoplanet and hence the increasing angular velocity demanded by conservation of angular momentum. Further outward transfer of angular momentum is expected during stage 3 as long as the nebula persisted, as discussed in more detail in Section V.

After the attainment of complete hydrostatic equilibrium that marks the beginning of stage 3, Saturn continued to contract, but at a very slow rate. This contraction occurred because the planet was radiating to space and because its interior was not totally incompressible. During the earliest portion of stage 3 ($\sim 10^6$ years), contraction took place sufficiently rapidly that the released gravitational energy caused a continued warming of Saturn's interior, despite the planet radiating to space at an intrinsic luminosity of 10^{-5} $L_\odot$, where $L_\odot$ is the Sun's present luminosity.

However, the interior became increasingly incompressible so that throughout almost all of stage 3 ($\sim 4.6 \times 10^9$ years), the interior underwent a progressive cooling (Pollack et al., 1977; Bodenheimer et al., 1980; Grossman et al., 1980). At the end of the interior warming phase, the central temperature was about 20,000 K, whereas at present it is about 10,000 K. During the entirety of stage 3, the radius and intrinsic luminosity steadily declined, achieving values that are 3 1/2 times and 4 1/2 orders of magnitude smaller at the present epoch than their corresponding values at the commencement of stage 3.

c. Present Internal Heat Source

As noted in Section II, Saturn radiates to space at present about 1.8 times as much energy as the amount of sunlight it absorbs. Here, we examine our current understanding of the source of the excess luminosity. Even when allowance is made for the presence of a heavy element core, the intrinsic luminosity that can be realized from the decay of long-lived radioactive isotopes of K, U, and Th falls short of the observed value by about two orders of magnitude (Flasar, 1973). Only gravitational energy release is capable of supplying the required intrinsic luminosity (ibid). The major question concerns the nature of the gravitational energy release. In particular, what are the relative roles of present gravitational contraction, present cooling of the interior that was warmed during earlier, more rapid contraction phases, and gravitational segregation, especially of He from H?

Detailed evolutionary calculations of Saturn during stage 3 have provided a partial answer to the above question. Figure 5 compares the observed intrinsic luminosities of Jupiter and Saturn with predicted values at a time of 4.6×10^9 years after the start of stage 3 (Pollack et al., 1977). These results are insensitive to the choice of initial conditions. They were obtained for homogeneous compositional models that lacked central heavy element cores. However, the predicted excess does not change significantly when a central core is included (Grossman et al., 1980). According to this figure, the observed intrinsic luminosity of Jupiter can be closely replicated, but the predicted value for Saturn falls short by about a factor of 3. About 1/3 of the predicted luminosity for both planets resulted from their present contraction rates, while the remaining 2/3 was derived from cooling of their interiors (Pollack et al., 1977).

In view of the success of the homogeneous model for Jupiter, it appears that its lack of success for Saturn is most likely due to gravitational segretation. Only He is sufficiently abundant for its separation from H to supply the needed deficit. As early as 1967, the importance of gravitational layering for generating internal energy in the outer planets was realized (Kieffer, 1967). Exploration of the physical processes by which this layering could occur were begun in 1973 by Salpeter and studied further by Salpeter and Stevenson (1977). According to Salpeter (1973), He could be expected to first become partially immiscible in H in the metallic H zone. While diffusion of He atoms occur too slowly, even over the age of the solar system, to release significant amounts of gravitational energy, rapid segregation could be realized through the nucleation of He droplets and their continued growth to droplet sizes characterized by large terminal velocities.

An explicit calculation of the temperature and pressure conditions required for He immiscibility to occur were made by Stevenson and Salpeter

(1977), who found that it would first begin in the outermost part of the metallic H zone when the temperature fell to ~10,000 K and that it would spread to progressively deeper regions of the metallic H zone with time. A major theoretical uncertainty at that time, and even today, is the nature of the phase transition from molecular to metallic H. If it is a first order transition, a density discontinuity occurs at the boundary between the two phases. As a result, He might not be exchanged effectively between the molecular and metallic zones, or some of the He removed from the upper part of the metallic H zone might be transferred to the molecular H region. An even more basic problem is the considerable uncertainty in the conditions under which He becomes immiscible in metallic H. According to MacFarlane and Hubbard (1983), the critical temperature, below which He becomes partially immiscible in metallic hydrogen, is a factor of about ten smaller than that found by Stevenson and Salpeter (1977). If so, no He separation would be expected in Saturn's interior and, thus, the source of its excess energy would not be understood.

The large discrepancy between the two estimates of the critical temperature for helium immiscibility stems from the need to know the Gibbs free energy of hydrogen-helium mixtures to an accuracy of much better than a percent. Unfortunately, such accuracy is very difficult to achieve. Stevenson and Salpeter (1977) used quantum mechanical perturbation theory to determine the Gibbs free energy, while MacFarlane and Hubbard relied on the Thomas-Fermi-Dirac (TFD) theory of high pressure materials. Because atoms are more strongly screened in the TFD theory than in the theory used by Stevenson and Salpeter, the critical temperature occurs at a lower value in the TFD theory. More accurate calculations are required to resolve this crucial discrepancy.

Salpeter (1973) proposed that the gravitational energy released by He immiscibility was the source of Jupiter's excess luminosity. Pollack et al. (1977) first pointed out that gravitational segregation was probably not operative for Jupiter, but was probably operative for Saturn. They based this conclusion on two points. First, their homogeneous contraction models were capable of reproducing Jupiter's observed excess luminosity, but not Saturn's, as pointed out above. Second, the temperatures in Jupiter's metallic H zone at present lie about a factor of 2 above the temperature at which immiscibility is first reached, according to Stevenson and Salpeter (1977), while this point is reached in their Saturn models after only about 1×10^9 years of evolution (cf. Fig. 6). They also pointed out that planet-wide segregation of He was required to produce the observed intrinsic luminosity. Hence, He had to be efficiently exchanged and uniformly mixed between the molecular H zone and the top of the metallic zone. They predicted that He is depleted in the observable atmosphere of Saturn by several tens of percent. Somewhat more refined estimates of this depletion factor of ~40% were obtained by Stevenson (1980) and Hanel et al. (1981). These values compare favorably with the apparent deficiency of He in Saturn's atmosphere deduced from the IRIS observations of Hanel et al. (1981), although the He mixing ratio in Saturn's atmosphere differs from that in Jupiter's atmosphere at only the 1+ standard deviation level.

There is a strongly coupled servo loop connecting He segregation, internal temperatures, and excess luminosity. The amount of He segregation occurring over any given time interval is determined by the drop in temperature that takes place in the metallic H zone. But this decrease is determined by the amount of excess luminosity radiated to space during this interval, which in turn is determined chiefly by the amount of gravitational energy released by He segregation. Thus, only as much He segregation occurs as is needed to self-consistently match the luminosity needs.

In summary, homogeneous contraction and thermal cooling appear to be inadequate sources of Saturn's excess luminosity, although they can fully account for Jupiter's excess luminosity. A plausible additional energy source is the gravitational energy released by the partial immiscibility of He in metallic H at low temperatures. The apparently observed depletion of He in Saturn's observable atmosphere, in comparison to solar elemental ratios and the He abundance in Jupiter's atmosphere, offers some evidence in support of this hypothesis. But the theoretical foundation for He immiscibility has been called into question by the thermodynamic calculations of MacFarlane and Hubbard (1982).

IV. Origin of Phoebe

There are several characteristics of Phoebe that suggest that this outermost satellite of Saturn is a captured object, rather than one that formed within the Saturn system during its early history. First, it has a retrograde orbit of high inclination and eccentricity, in contrast to all the other satellites. Second, as discussed in Section II, its low visible albedo and spectral reflectivity properties stand in marked contrast to the corresponding properties of the other satellites of Saturn, but are similar to those of carbonaceous chondrites, the irregular satellites of Jupiter, Jupiter's Trojan asteroids, and C type objects in the asteroid belt. Indeed, if Phoebe formed within the Saturn system, we would expect it to be at least as rich in ices as the other satellites, given its greater distance, rather than essentially ice free.

There are three major classes of capture theories: Lagrange point capture, collision between a stray body and a natural satellite, and gas drag capture. According to the first of these, a body initially in orbit about the Sun can transfer to an orbit about a planet by passing at very low velocity relative to the planet through its interior Lagrange point (Heppenheimer, 1975). However, as can be seen from the symmetry of the equation of motion with respect to the sign of time, such capture is only temporary, with the body returning to a solar orbit through the Lagrange point after only a few or at most about a hundred orbits about the planet (Heppenheimer and Porco, 1977). Permanent capture could occur if Saturn's mass increased by several tens of percent or if the Sun's mass decreased by a comparable percentage during the time of temporary capture (1-100 years) (ibid). However, no such rapid change in either body's mass is predicted by current theories of the formation of the solar system. For example, the calculations of Safronov and Ruskol (1982) for the core instability model have time scales of $\gtrsim 6 \times 10^4$ years during which Saturn's mass increases by several tens of percent (cf. Table 2). Until plausible mechanisms for effecting permanent capture are proposed, the Lagrange point mechanism cannot be viewed as an entirely satisfactory theory for the capture of Phoebe.

Colombo and Franklin (1971) suggested that the two families of irregular satellites of Jupiter originated from the collision of a stray body with a regular satellite of this planet, with the prograde irregular satellites being fragments of the original satellite and the retrograde moons being fragments of the stray body. One potentially serious problem with applying this theory to Phoebe is the absence of a larger <u>irregular</u> satellite of Saturn having a prograde orbit (recall that Phoebe has a retrograde orbit). Also, no other satellite of Saturn is made of the same material as Phoebe.

Early theories for gas drag capture of satellites were advanced by See (1910) and Kuiper (1951). Pollack et al. (1979) presented a modern version of this theory that took into consideration the evolutionary phases of the outer planets discussed in Section III. According to this latter model, Phoebe formed independently in the outer solar system by accretional processes and was captured at the very end of stage 1 (early hydrostatic) when it passed through the outer portion of proto-Saturn and had its relative velocity reduced by gas drag. Under most circumstances, gas drag would continue to act on the captured body and it would soon spiral into the center of the protoplanet to be incorporated into its core. This may, in fact, have been the fate of many other stray bodies that were captured at less opportune times. However, the onset of the hydrodynamical collapse shortly after Phoebe's putative capture quickly removed gas from the body's orbit, thus allowing it to remain a satellite and permitting its orbit to retain a significant eccentricity and inclination. Capture within about 10 years prior to the start of stage 2 is required to achieve this end state.

Several predictions of the gas drag theory can be compared with the observed properties of Phoebe. First, its semimajor axis should be comparable to or somewhat less than the radius of proto-Saturn at the onset of the hydrodynamical collapse. For the gas instability model, stage 2 begins at a radius of $\sim 60\ R_S$ for a spherically symmetric protoplanet (Bodenheimer et al., 1980). A somewhat different value may characterize a protoplanet having a non-zero angular velocity. For the core instability model, the corresponding radius is equal to the tidal radius or $\gtrsim 125\ R_S$, where the equality holds if the Sun had already formed. Also, in accord with Mizuno's (1980) calculation, we might assume that the protoplanet had a mass of ~35 $M_\oplus$ at this time. If so, subsequent growth to the planet's present mass would have caused the captured satellite's orbit to decrease by a factor of ~3. The above estimates of the outer boundary of proto-Saturn at the commencement of stage 2 do not appear to be inconsistent with Phoebe's semimajor axis, 215 R_s. In the case of the core instability model, it may be necessary for the Sun not to have fully formed at the time of stage 2 in order for Phoebe to achieve, ultimately, its present orbital distance.

Phoebe's radius of 110 km (Smith et al., 1982) may be compared with the range of sizes for which gas drag capture would be effective. A stray body has to pass through an amount of nebular mass that is at least ~10% of its own mass in order to be significantly slowed down (Pollack et al., 1979). Also, the captured object cannot be too small or else it would be carried along by gas drag during the collapse phase. Using Bodenheimer's (1977) model of proto-Jupiter near the end of stage 1 and scaling this to proto-Saturn, Pollack et al. (1979) predicted that bodies having radii between 0.1 and several hundred kilometers could be captured by proto-Saturn and survive as satellites. The observed size of Phoebe is consistent with this rather broad range of sizes.

The above discussion indicates that Phoebe was most likely captured by gas drag, although this theory is far from proven. Let us for the moment accept this theory as being correct and consider its consequences. First, asteroid sized bodies were present in the outer solar system close (~10^6–5×10^6 years) to the times at which Jupiter and Saturn originated. Presumably, these bodies formed through accretional processes. This deduction lends credence to, but does not prove, the core instability model for the origin of the giant planets. Second, the number density of planetesimals near Jupiter and Saturn's orbits at these early times may have been similar, since each planet captured one, several hundred kilometer-sized, stray body (in Jupiter's case, this was the parent body of the prograde satellites, which fragmented into these satellites, due to dynamic gas pressure (cf. Pollack et al., 1979)). Third, temperatures within the solar nebula at these times may have favored the formation of carbonaceous chondrite-like material near Jupiter's and Saturn's locations. While as much as several meters of water ice could have been ablated off the leading side of Phoebe during the capture process, ice located at greater depths would have been excavated by cratering events at subsequent times and brought to the surface to significantly brighten it. This expectation is inconsistent with Voyager 2 pictures of Phoebe, which show its surface to be very dark (Smith et al., 1982). Therefore, the presently observed surface composition of Phoebe was not significantly altered by the capture process.

V. Origin of the Satellite System

As discussed in Section III, gravitational energy released by contraction during the first 10^6 years of the late, quasi-hydrostatic stage provided Saturn with a luminosity of 10^{-5} $L_{\odot}$. This planetary luminosity together with viscous dissipation in the nebula preferentially heated the inner portions of the satellite nebula, which formed during the short-lived (~1 year) hydrodynamic stage. One can construct models of the evolution of this nebula; by seeing which classes of models produce satellites consistent with their observed properties (e.g., composition, size), one can derive constraints on the nature of the nebula (e.g., temperature structure, lifetime).

Such modeling must examine three phases in the history of the satellites: the equilibration of solids with the gas, to determine the chemical composition of the material from which the satellites were formed; the accretion of these solids into satellites; and the thermal and geological evolution of these satellites after their accretion. This last phase, which is treated in Section VI, is not only interesting in its own right, but also necessary if we wish to use characteristics of the satellites as observed today to constrain the conditions in the regions where they were formed 4.6 billion years earlier.

Lewis (1972) examined in detail the chemical species which would exist in local thermodynamic equilibrium in a gas of solar elemental composition at low temperatures and a variety of pressures. In contrast to the higher temperature conditions prevailing in the inner part of the solar nebula, ices as well as "rocks" could have condensed in the outer portion of the solar nebula and in portions of the nebulae of the outer planets. An examination of how these phases could be assembled into icy bodies was presented in Consolmagno and Lewis (1977). Figure 7 shows the results of Lewis' chemical equilibrium model, outlining the regions of stability of various ices in pressure-temperature space. In general, water ice is the highest temperature ice condensate and is the most abundant ice species, since oxygen is more abundant than carbon or nitrogen in a gas of solar elemental composition. At sufficiently high pressures or low temperatures, water occurs instead in solution with ammonia monohydrate, either as a liquid (high pressure) or solid solution (low temperature). In the presence of condensed water and at temperatures significantly below those at which water first condenses, gaseous methane forms a clathrate, effectively exhausting the available water; the remaining methane freezes out at very low temperatures.

The above results are significantly altered if nonequilibrium species, formed at higher temperatures or conceivably in regions of nonsolar chemical abundances, survive at these low temperatures. Lewis and Prinn (1980) showed that CO and N_2, the stable carbon- and nitrogen-bearing species in the warmer parts of the solar nebula, could be kinetically stable for times comparable to the age of the solar nebula against reactions that convert them to methane and ammonia in the outer solar nebula. If there were large scale convection throughout the nebula, gas carried into the warm regions and converted into CO and N_2 would not have time to change back into CH_4 and NH_3 when it was carried back into the colder, outer regions. Thus, in the outer solar system, out to the regions where comets reside today, one would expect, for example, CO ice rather than methane ice.

However, in circumplanetary nebulae, the situation may be different. If the gas pressure is sufficiently high, methane and ammonia may be stable at temperatures sufficiently high to allow reactions forming these species from CO and N_2 to go to completion on time scales much less than the lifetime of the nebula (10^6-10^7 years), especially in the presence of dust grains which could act as catalysts. Prinn and Fegley (1981) examined this question with regard to the circum-Jovian nebula, and concluded that methane and ammonia gas could well be formed there; pressures were sufficiently high so that kinetic inhibition would not have been a problem, although N_2 and CO may have also been present there in nontrivial amounts.

An important question to be addressed, then, is the pressure and temperature structure of the Saturnian nebula. This will tell us what chemical constituents were present within the nebula, and whether or not kinetic inhibition of certain species might have been important.

The satellites themselves put limits on the mass of the nebula. An obvious minimum mass is the mass of the satellites, plus sufficient gas to bring the condensed material into cosmic elemental abundance, with hydrogen and helium being the most abundant gas species. To obtain an upper limit we will assume that the nebula was not more massive than Saturn itself. Given cosmic abundances (e.g., Cameron, 1973), the mass of condensibles in a low temperature (~50-250 K), solar composition nebula is about 1% of the total mass; thus, multiplying the mass of the satellites by 100, we find the minimum nebula mass is of the order of 10^{28} g, while the maximum mass is of the order of 10^{30} g. Spread uniformly in a disk as thick as Saturn and extending to the orbit of Iapetus, the density of the nebular gas lies between 10^{-3} and 10^{-5} g/cm^3. These densities imply pressures of the order of 0.1 to 10 bars, for a temperature of 200 K. (Considering a smaller minimum mass nebula extending only out to Rhea, using the masses of the inner five regular satellites and neglecting Titan, one finds a similar nebular density.) Even the minimum mass nebula would have been much more dense than the solar nebula in the region of the outer planets.

Of course, one would expect density, pressure, and temperature to be higher near Saturn, and lower farther out in the circum-Saturnian nebula. Exactly how these quantities vary with position is model dependent, however.

The dependence of nebular pressure P, density ρ, and temperature T on radial distance r, vertical distance above the midplane z, and time t is determined by force balances and energy transport in the r and z directions. To a very good approximation, hydrostatic equilibrium determines the variation of ρ with z, with the vertical component of gravity balancing the vertical component of the pressure gradient. Note, however, that the latter might include a nonnegligible component due to turbulence having a characteristic velocity not much smaller than the speed of sound. Thus, the pressure scale height, H, is proportional to $r^{3/4}T^{1/2}$ (Lin, 1981; Lunine and Stevenson, 1982). For typical values of T, $H \cong 0.1r$. In the radial direction, the key forces are gravity (mostly Saturn's), centrifugal force, the radial component of the pressure gradient, and Reynolds stresses due to viscosity. In many cases, the first two forces are the dominant ones, although, as indicated below, viscous dissipation may play a key role in the evolution of the nebula.

There are two major sources of heating for the nebula: the heat emitted by Saturn and that produced by viscous dissipation. When Saturn's luminosity controls the temperature structure of its nebula, the dependence of T on r and z is determined by the opacity of the nebula. If the opacity is small, $T \sim r^{-1/2}$ and is approximately independent of z (Pollack et al., 1977). In this case, individual particles are in radiative balance with Saturn's luminosity and help to heat the surrounding gas. When the nebular opacity is large in both the r and z directions, the radiative equilibrium temperature gradient is likely to be convectively unstable, leading to $T \sim r^{-1}$ and similarly T decreases steeply with increasing z. Naturally, at large enough values of r and z, the opacity becomes small and hence subadiabatic temperature gradients are achieved, with the temperature asymptotically approaching that of the surrounding solar nebula. When small grains of ice and silicate are present in the Saturnian nebula, as they would be during most of its lifetime, they serve as the dominant source of opacity and insure that the inner portions of the nebula near its midplane are optically thick in both the r and z directions. Even in their absence, the nebula is optically thick in the radial direction and perhaps even in the z direction due to the pressure induced transitions of hydrogen that are effective at the high pressures of the nebula (Lunine and Stevenson, 1982).

During the last several years, it has become fashionable to apply the concepts of viscous accretion disks around stars (Lynden-Bell and Pringle, 1974) to models of the solar nebula (e.g., Cameron, 1978; Lin and Papaloizou, 1980; Lin, 1981). Conceivably, these concepts are also relevant to nebulae around the outer planets, although to date only Lunine and Stevenson (1982) have used them for the Jovian nebula. In such models, viscous dissipation within the nebula plays a central role in heating the nebula and in causing it to evolve with time. Unfortunately, the source of the viscous dissipation and the relationship between the kinematic coefficient of viscosity and other state variables have been key problems for these models. But Lin and Papaloizou (1980) and Lin (1981) have suggested that thermal convection in the vertical direction is the dominant source of the turbulence that leads to viscous dissipation and have used mixing length theory to explicitly determine it. According to these calculations, $T \sim r^{-3/2}$ in the inner, opaque portions of viscous accretion disks. Since the implied temperature gradient in the radial direction is superadiabatic for the solar nebula and nebulae of the outer planets, it is possible that thermal convection in the radial direction may result, in which case a $T \sim r^{-1}$ relationship would be established. But the rotation of the accretion disk may hinder the occurrence of thermal convection in the radial direction, in which case the $T \sim r^{-3/2}$ relationship may be maintained.

Due to viscous dissipation, the mass distribution of the nebula varies secularly with time. In particular, there is an inward directed mass flux and an outward direction flux of angular momentum. Thus, the mass of the nebula decreases with time as the central object (e.g., the Sun or Saturn) accretes inflowing material. Also, the outer parts of the nebulae expand due to the outflux of angular momentum. A typical lifetime for a viscous accretion disk model of the solar nebula is about 10^5 years (Lin, 1981). Analogous lifetimes for nebulae of the outer planets could well be much shorter, on the basis of a simple scaling of formulae given by Lin (1981). If so, it is not clear that satellites could be assembled in so short a time scale.

In summary, viscous accretion disks differ in their properties in the following ways from optically thick disks, whose temperature structure is controlled by the central object's luminosity: a superadiabatic temperature gradient (vs an adiabatic one) may be present in the inner parts of the nebula. The temperature of the disk may be semidiscontinuous (vs continuous) near the central object's photosphere; the total mass and mass distribution in the nebula continuously vary with time (vs are nearly constant); and the lifetime of the nebula may be very short, $\ll 10^5$ years (vs 10^6 years).

In all published papers to date concerning the Saturnian nebula, only models for which the planet's luminosity is the dominant heat source have been investigated. Thus, of necessity, the detailed discussion given below reviews nebula models based on this type of heat source.

The first explicit calculation of the temperature structure of a Saturnian nebula and the history of condensation products in it was made by Pollack et al. (1977). They considered two limiting cases in evaluating the variation of temperature with radial distance in the nebula: optically thick and thin nebulae. As discussed above, $T \sim r^{-1}$ in the former case and $T \sim r^{-1/2}$ in the latter case.

Figure 8 illustrates how temperature varies with time and distance in the high-opacity case (the more likely situation during the early phases of the nebula, before grains underwent successive aggregation). Because Saturn's luminosity decreased with time during the late, quasi-hydrostatic stage, a given ice species first condensed at progressively later times at closer distances to Saturn. Thus, satellite and ring formation need not be coeval throughout the nebula. For the sake of simplicity, we will assume below that condensation of satellite-forming material occurred at some discrete time, which can be characterized by a single radial temperature profile. This time may be the last, coldest epoch of condensation, just prior to the dissipation of the nebula. But the possibility that satellites formed at different times should be kept in mind.

A lower limit for the lifetime of a nebula heated by Saturn's luminosity can be derived from Figure 8 by finding the time at which ices first condensed at a given location. Water ice first condensed in the region of the B ring at 10^7 years from the end of the hydrodynamic collapse phase and methane clathrate first formed at Titan's distance at 10^6 years.

Prentice (1980, 1981) developed an elaborate theory of the physics of the Saturnian nebula, from which temperatures and pressures in satellite-forming gas rings could be determined. Of necessity, however, his theory was based on many assumptions concerning initial conditions and the behavior of the gas-dust mixture as the nebula evolved. Some parts of his formalism, most notably supersonic turbulence within the nebula, are quite controversial and, indeed, appear to be implausible.

Weidenschilling (1982) developed a model for the temperature and pressure structure of the nebula by assuming that the mass distribution in the nebula was in some way reflected by the distribution of mass in the satellites today. Given a distribution of nebular density, one can then find a pressure profile either by solving for a hydrostatic, rotating gas disk or by assuming the nebula was convecting and adiabatic.

Weidenschilling (1982) used the formalism of Safranov (1972) for evolving nebulae for which rotational and gravitational energies were in balance, and applied the resulting relationship between temperature and distance from the nebula center to a nebula massive enough to produce the Saturnian satellites. The Safranov relationships neglect disk self-gravity, and lead to a temperature gradient in the nebula which is subadiabatic, and hence stable against convection. Such a shallow temperature gradient seems unlikely in view of the large grain and gas opacities in the radial direction, as discussed above.

Alternatively, one can follow the work of Prinn and Fegley (1981) for Jupiter, and Pollack et al. (1976) for Saturn and assume that the nebula was convecting and adiabatic. The density of the nebula can be assumed, or taken from the surface density, whose variation in space can be defined by the $1/r^{2.5}$ trend seen for Tethys, Dione, and Rhea in Figure 9. If one assumes that the position of Mimas coincided with the condensation of water ice, the temperature and pressure at that position can be determined, and an adiabatic gradient followed out to the position of Rhea (cf. Table 3). Beyond Rhea, such an adiabat would predict temperatures lower than the ambient temperature at Saturn's distance from the Sun; the nebula thus might be presumed to be isothermal beyond that point.

In general, one can postulate a wide variety of Saturnian nebula models. There still does not exist any generally accepted theory describing the evolution of such disks of gas, nor is there even agreement as to the proper set of starting conditions. But in nearly all of the above models of the nebula a similar condensation sequence results. Rocky material plus water ice are assumed to be stable at the positions of Mimas and Enceladus; ammonia monohydrate is also present at the distances of Tethys and Dione, with methane clathrate possible at Rhea's location and likely at Titan's and Iapetus'. Such a pattern is illustrated in Figure 7, where the left-hand curve marks an adiabat of a minimum-mass nebula as described above. The right-hand curve signifies a maximum-mass adiabat, which represents a significantly different condensation scheme. There, ammonia monohydrate is present even at Mimas' and Enceladus' distance.

Once solid material has condensed in a circum-Saturnian nebula, it settles into the midplane of the nebula, collects itself into rings, and eventually accretes into planetesimals, from which the satellites, in turn, are accreted. Analytical and numerical models of this process have been developed, most recently by Weidenschilling (1981) and Coradini et al. (1981), looking specifically at the case of accretion in nebulae of the outer planets.

As we saw above, the gas densities in such nebulae are much higher than in the solar nebula; thus, gas-dust dynamics are likely to be quite important. Gas drag, which causes an inward spiraling of particles, leads to very rapid evolution times for accretion of dust to planetesimals. Consequently, one expects rapid and efficient accumulation of satellites in the nebula. In this situation, satellite formation is bounded by the time scale over which Saturn's luminosity decreased significantly or the viscous dissipation lifetime of the nebula. Satellites could have formed with a zoned structure if the accretion time scale is much less than the latter time scales, with the lower temperature condensates being located closer to their surfaces (cf. Consolmagno and Lewis, 1977).

In such a straightforward nebula, satellite masses might be expected to reflect the mass of material available in the nebula, and the bulk chemical properties of each satellite to be fixed by the local pressure and temperature conditions. The distribution of mass within the Saturnian satellite system is quite irregular, however, especially in contrast to the Galilean satellites of Jupiter, as noted by Weidenschilling (1982). He took the masses of each satellite, augmented them by sufficient material to include the mass of uncondensed gas, spread these masses into annuli centered on the orbits of each satellite, and thus determined nebular surface density as a function of distance from Saturn. This is illustrated in Figure 9.

Figure 9 also includes the results of the exercise for the Galilean satellites. In that case, a monotonic and basically linear decrease in density is seen. Such a decrease is also seen for Tethys, Dione, and Rhea, but Mimas and Enceladus are much too low in mass, and Titan much too massive, for this simple gradation of densities.

Weidenschilling (1982) suggested that aerodynamic effects separating the first-condensed materials in the dense proto-Saturnian nebula may be responsible for the reduced masses of the inner two satellites, similar to his explanation (Weidenschilling, 1978) for the small mass and high density of Mercury compared with the other terrestrial planets. Alternatively, Pollack et al. (1976) pointed out that the commencement of satellite formation in the innermost region of the nebula may have been delayed, due to the high initial temperatures there and the large initial size (3-5 R_S) of Saturn. Moons that began accreting early (e.g., Tethys, Dione, and Rhea) may have accreted more efficiently due to their larger sizes than ones that began later (e.g., Mimas and Enceladus). Finally, these satellites may simply be fragments of initially larger bodies, broken up by cataclysmic collisions (cf. Smith et al., 1981).

The case of Titan presents the opposite problem. Prentice (1981) suggested that Titan was a planetesimal from the solar nebula which was captured by Saturn. No mechanism has yet been worked out, however, which could bring such a massive body from a solar orbit into a regular, circular, noninclined, prograde orbit about Saturn (cf. the discussion in Section IV concerning the possible capture of Phoebe).

Alternatively, one might speculate that Titan is the only survivor of an accreting satellite system which underwent intense bombardment and disruption of accreting planetesimals. A 10 km radius comet impacting at a relative velocity of 10 km/sec (a typical orbital speed for inner Saturnian satellites) would have sufficient energy to shatter a 2500 km radius icy moon (cf. Greenberg et al., 1977). Such impacts would have to be much more common at Saturn's distance from the Sun than at Jupiter's during the period of satellite formation to account for the survival of the four Galilean satellites. However, the Valhalla basin of Callisto shows that large impacts did occur in that system, and such impacts would be less likely to shatter Ganymede if they occurred when that moon was significantly melted. Another difficulty with the above catastrophic disruption hypothesis is that the moons other than Titan represent collectively only about 10% of the mass of Titan. If they are survivors of a family of Titan-class objects, a significant amount of their original mass must have been broken into very small fragments that were lost from the system via plasma drag, gas drag, or sublimation, perhaps to be captured eventually by Saturn or by Titan itself.

Given the chemical trends predicted by the work described above, one would expect to see a regular and predictable trend in satellite bulk densities, just as occurs for the Galilean satellites of Jupiter. But there is no pattern to the densities of the Saturnian satellites (cf. Fig. 1). In part, this difference between the two satellite systems may reflect the more numerous types of ices possible in the Saturnian system than near Jupiter and the occurrence of a major ice component throughout the Saturnian system. There is much less of a density contrast among various ice species, as may occur for the Saturnian system, than for varying mixtures of rock and water ice, as occurs for the Jovian system. In addition, the large uncertainties in the densities of Mimas and Enceladus make it difficult to draw hard and fast conclusions about trends in density. But it is clear that Tethys is less dense, and Dione more dense, than a theory of simple condensation and accretion would predict.

This lack of regularity has led to suggestions that the satellites we see today may be reaccreted fragments of protosatellites which were broken up during an early period of heavy bombardment. Smith et al. (1980) noted that the cratering flux implied by the densely cratered plains on Iapetus and Rhea should have led to at least some impact events, deeper in Saturn's gravity well (i.e., in the inner satellite system) violent enough to completely disrupt these moons; and, indeed, both Mimas and Tethys have an enormous crater on their surface whose impact energy must have been very nearly sufficient to accomplish such a disruption. Note, however, that this argument depends on an extrapolation to larger sizes of the population of impacting bodies responsible for the craters on Iapetus and Rhea.

What if the first moons formed were disrupted into a few large chunks? Random reaccretion of such chunks could account for the deviations of satellite density from a regular pattern. It can be shown that treating the densities of Tethys and Dione as one-sigma deviations from a mean density would imply that they would have been assembled from only 30 or so planetesimals of pure rock or ice. Indeed, fragmentation experiments on ice (though clearly not of planetary size) show that the largest fragments are on the order of 1/30 of the original mass. Thus, superimposed on a radial variation of the proportion of low temperature ices, there may be a random component of varying amount of rock and ice.

VI. Evolution of the Regular Satellites

a. Interior Evolution

Given the composition of the satellites, as implied by the models of the previous section, one can construct evolutionary models of them and test their behavior against the observed surface features of the satellites. Such models attempt to predict the temporal and radial variation of temperature, composition, and size of the satellites' interior, which are determined by the strength of heat sources, bulk composition, size, and initial conditions. Key heat sources for the Saturnian satellites, as for the Jovian ones, include gravitational energy released during satellite formationary (accretional heat), radioactive decay of long-lived radionuclides (U, K, and Th) contained in the "rock" or "silicate" component, and tidal friction. The buildup or loss of heat from the satellites' interiors is controlled by liquid and solid state convection as well as ordinary solid state conduction. Thus, the smaller satellites evolve more quickly than the larger ones, in cases where tidal heating is unimportant, to thick crusts and cool interiors and hence "geologically dead" surfaces. Tidal heating can be important for satellites that are situated close to their primaries and have large, forced eccentricities. In such cases, even small satellites can remain geologically active over much of their lifetime.

Constraints on thermal history models and hence on properties of the satellites' interior are placed by the observed morphology of their surfaces. Tectonic features provide markers of epochs of increases or decreases in the size of satellites due to phase changes and/or compositional segregation occurring in their interiors, while resurfacing events denote times when near surface liquids have been able to reach the surface. Crude time markers for these features are provided by the density of craters on them. All of the large satellites of Saturn, whose surfaces have been photographed at good spatial resolution (i.e., Mimas, Enceladus, Tethys, Dione, and Rhea), have experienced both extensional tectonism and resurfacing, although the timing and extent of these processes have varied greatly among these inner five satellites. The occurrence of a thick atmosphere, which obscures its surface, and its large size imply a geologically rich history for Titan. Iapetus' surface has not been photographed at an adequate resolution to define its surface geology, although its comparatively large size would, by analogy to Dione and Rhea, suggest that its surface has undergone some tectonism and resurfacing.

The first evolutionary models for the Saturnian satellites were developed by Consolmagno (1975), who computed the time-dependent flow of heat from small icy moons with a cosmic composition of rock, water, and ammonia. Heating was due to the decay of radioactive nuclides in the rocky material; heat transport was by conduction within the ice, and convection within melted ammonia-water regions. This work was further developed in Consolmagno and Lewis (1978), who noted that the small icy moons of Saturn would probably not be stable against solid state convection.

The first thermal model to explicitly include solid state convection in outlining the evolution of Saturn's satellites was that of Ellsworth and

Schubert (1982). Ellsworth and Schubert (1983) constructed models for bodies of water ice and silicates but with no ammonia or methane and hence no eutectic melting. They proposed that the presence or absence of solid state convection could be the deciding factor in determining whether tectonic features appear on the surfaces of these satellites. According to their models, only Dione and Rhea would have experienced substantial convection; these are the two moons with the most widespread extensional features (neglecting Enceladus, which presumably was subjected to tidal heating and is not, therefore, included in these models). But it is not clear why solid state convection would produce only extensional, but not compressional, tectonic features nor whether the occurrence of a limited amount of extensional tectonic features on Tethys and Mimas is consistent with the behavior of these models.

One major issue suggested by their work is the need for a quantitative estimate of the surface stresses which would result from the predicted internal convection. The first step, an estimation of the velocities in convecting icy satellites, has been taken by Golitzyn (1979) but connecting these velocities with surface features remains to be carried out.

A different approach to the problem of the origin of surface tectonic features is to examine the stresses produced as these moons expand and contract upon heating and cooling. Such stresses would be greatest where phase changes occur inside these bodies.

As a first step in such modeling, Consolmagno and Huang (1982) constructed thermal models of five of the large regular Saturnian moons; they used Voyager II masses to define the moons' mean densities and explicitly examined the density changes of the various components upon heating and cooling. Enceladus, which clearly has been resurfaced in the recent past, presumably has a special heating source, such as tidal heating (see below), and so it is excluded from this thermal model; Titan, which is massive enough to contain mostly high pressure phases, represents a separate problem as well. In the first case considered, the satellites were assumed to be made of water and rocky material only (no ammonia), whose relative abundances were determined from the observed mean densities. Two sets of models were investigated: one in which these bodies formed slowly enough so that they were initially a cold (~80 K), homogeneous mixture of water ice and rock; and one in which they accreted quickly enough so as to start their histories fully differentiated, with liquid water mantles overlying rocky cores.

These two sets of models fail to provide expansion after the first 100 million years, and fail to provide interior temperatures warm enough to melt ice or to keep water liquid for very long (cf. Table 4). But Dione and Rhea are observed to have lightly cratered extensional features, which are, presumably, at least a billion years younger than the oldest surfaces of these satellites; some evidence of resurfacing by liquid material also exists in this time frame. Thus, these models are inconsistent with the satellites' surface morphology.

The most severe shortcoming of these models, as well as that of Ellsworth and Schubert (1983), is that they neglect the presence of ammonia monohydrate, which is expected in many or all of these satellites (depending on conditions in the nebula, as described in Section V). A more complex model has been constructed by Consolmagno (1983), based on the model of Consolmagno (1975) which did include ammonia eutectic melting, but which was limited at the time by a lack of information on the masses and sizes of the satellites in question. This model was expanded to include changes in radius due to changes in density as ice melted and as the composition of the melt changed (with the addition or freezing out of water). The mean density of each satellite was matched with a composition including rocky material of density 3.0 g cm^{-3}, ammonia monohydrate, and water ice, with the latter two having jointly cosmic proportions of N to O. The initial conditions for this model corresponded to those appropriate for slow accretion: a temperature everywhere of 80 K and a uniform distribution of rocky material.

The above model succeeded in matching some of the surface morphology inferred for these bodies from the Voyager images (cf. Table 4 and Fig. 10): The model of Tethys showed a small degree of tectonism, while the models of Dione and Rhea showed evidence for extensional stresses and the possibility of flows on their surfaces. The presence of a low density, eutectic melt having a low freezing point (~170 K) and the passages opened by large-scale expansional stresses combine to favor the formation of surface flows. Surface extensional stresses of 25 bars for Dione and 60 bars for Rhea were obtained; the critical stress for extensional failure of ice at 80 K is not well known, but is probably on the order of 20 bars.

Another satisfying match of this model to observation is the time scale of such activity: well past the period of early heavy bombardment, but early enough to allow cratering by a later population of impactors. In this sense the evolution is comparable in time scale to that of the emplacement of mare material on the Earth's Moon. However, this model does not explain all the observed features on these satellites, including the large Ithaca Chasma on Tethys (which may be of impact origin (McKinnon, 1982; Moore and Ahern, 1981)), and areas that appear to be resurfaced on Tethys and Mimas (Plescia and Boyce, 1982). Also, the model predicts a greater resurfacing for Rhea than for Dione; in fact, the opposite is observed.

Variations on this model do not yield markedly better results. If the initial temperatures inside the bodies are raised, melting may occur somewhat earlier, but neither the degree nor the duration of the melting is substantially different from the models that start at 80 K everywhere. This is not surprising, since these moons are small enough to reach thermal equilibrium very rapidly. There is not a significantly long time lag between the production of heat in their interiors and its transport to the surface, and, hence, any thermal spike introduced into these bodies is soon conducted away.

Satellites that were initially differentiated into rocky cores and icy mantles could result from rapid accretion, due either to their being completely melted by accretional heat or being assembled in an "onion layer" fashion (Consolmagno and Lewis, 1977). Models run with such starting conditions predict roughly twice the contraction and expansion of Rhea as occurs for the model with homogeneous starting conditions; the times when these stresses appear remain the same. A model of an initially differentiated Dione shows a surface evolution very similar to the homogeneous case. However, an initially differentiated Tethys model is virtually the same as the corresponding Dione model. Given that such a starting condition would imply a Rhea that expands much more than Dione, and a Tethys indistinguishable from Dione, both in contradiction with observations, we conclude that such models seem less satisfactory than models starting with a homogeneous mixture of rock and ice.

Conceivably, models that lie between the extremes of being initially fully differentiated and fully undifferentiated might yield a better match to the observations. For example, such models might display sufficient expansion and near surface melting for Tethys to be compatible with its surface morphology, while at the same time implying a more active geology for Dione during its first ~10^9 years than for Tethys.

Coradini et al. (1982) also modeled the time-dependent melting of these satellites. They included the effects of ammonium monohydrate in producing a eutectic melt, as did Consolmagno (1983), but in addition incorporated the heating implied by their accretion models. As of this writing, this work remains in progress.

Models of Enceladus and Titan need separate, special treatment. As discussed in Section II, portions of the surface of Enceladus have been subjected to extensional tectonism and resurfacing over much of its history, with its youngest surfaces being less than about 1×10^9 years old. Squyres et al. (1983) proposed that the tectonism was the result of the freezing of liquid water (recall ice I is less dense than liquid water), and that the resurfacing was due to the eruption of a liquid NH_3/H_2O mixture onto the surface from a hot interior. Their suggestion that the resurfacing agent was a mixture of NH_3 and H_2O rather than pure water was motivated by the lower melting point of the mixture (as much as 100°C) and by the density of a eutectic mixture being less than that of solid water ice, thus facilitating the ability of the eutectic mixture to reach the surface. In contrast, liquid water is denser than solid water ice.

It is quite possible that resurfacing events on Enceladus are occurring even at the present epoch: The peak density of the E ring is located very close to the orbit of Enceladus (Brown et al., 1981), implying that Enceladus is the source of the particles in the E ring. In addition, the lifetime of the micron-sized particles of this ring is quite short (~10^3 years; Cheng et al., 1982). Hence this material must be constantly replenished, unless the E ring is a transitory feature.

The above discussion implies that the interior of Enceladus has contained liquid zones in its recent past, including perhaps the present, as well as at other times in its lifetime. But significant fluctuations in the size of these zones over its lifetime are implied by the presence of extensional tectonism, if solidification of liquid water is responsible for the satellite's expansion. As a result of Enceladus' small size and high bulk ice content, radiogenic heating fails by at least two orders of magnitude to provide the heating necessary to keep ices molten over much of the satellite's lifetime (Squyres et al., 1983). Indeed, if radiogenic heating was capable of meeting this requirement, it would even more easily cause extensive interior melting of the interiors of the larger satellites Tethys, Dione, and Rhea, contrary to observation.

The most likely source of the required heating of Enceladus is tidal dissipation engendered by the satellite's forced eccentricity (Yoder, 1979), just as tidal heating is suspected to be responsible for the active volcanism on Io. But there are quantitative problems with this mechanism for the current epoch. At present, Enceladus has a forced eccentricity of only 0.0044 due to a gravitational orbital resonance with Dione. Using this eccentricity and as low a tidal Q as seems likely ($Q = 20$), Squyres et al. (1983) obtained a tidal heating rate for a homogeneous, solid Enceladus that was comparable to the radiogenic heating rate and thus incapable of melting the satellite. Furthermore, for the same material properties, Mimas was found to have a tidal heating rate that was 30 times that of Enceladus, contrary to the strong differences in the ages of the surfaces on the two satellites.

Squyres et al. (1983) overcame the above difficulties faced by the tidal heating mechanism by proposing that Enceladus was initially melted by tidal friction at a time when the satellite's forced eccentricity was a factor of 7 to 20 higher than its current value and hence tidal heating was a factor of 50 to 400 times larger than at present. Furthermore, they point out that a much smaller tidal heating rate is needed to maintain a molten interior once it is established, since tidal dissipation for a thin, rigid shelled object is generally much larger than for a totally solid object. Minimum eccentricities ranging from the current value to seven times this value are adequate for maintaining a molten zone, depending on the composition of the melt (H_2O vs NH_3/H_2O) and on the thermal conductivity of the outer rigid shell. If the thermal conductivity of pure solid water ice is used, minimum eccentricities of five to seven times the present value are required. But if the thermal conductivity is about an order of magnitude smaller, due to the presence of hydrates and clathrates, and/or a frost insulating layer on the surface, minimum eccentricities close to the present value may be adequate. The failure of tidal heating to keep the interior of Mimas molten over most of its history can be attributed to a combination of different material properties (e.g., a higher thermal conductivity) and the absence of an earlier, higher forced eccentricity.

An intriguing mechanism for generating a higher forced eccentricity in the recent past for Enceladus has been suggested by Lissauer et al. (1983). They point out that Janus is quite close to a 2/1 orbital resonance with Enceladus. Furthermore, Janus' orbit should be evolving rapidly outward due to angular momentum it is exchanging with the main rings by means of spiral density waves. Hence, only 10^7-10^8 years ago Janus may have been temporally locked in a 2/1 resonance with Enceladus. In this case, the exchange of angular momentum between the rings and Janus would have resulted in a pumping up of Enceladus' eccentricity to a high enough value to have caused a melting of its interior. This resonance lock may have been broken either by a catastrophic collision or by the establishment of the resonance between Enceladus and Dione. In summary, tidal heating appears to be responsible for the occurrence of molten zones inside Enceladus over much of its lifetime, including perhaps the present epoch. A larger forced eccentricity than the present value is required to initiate melting. This may have occurred due to the transfer of angular momentum from the rings to Janus to Enceladus. Smaller eccentricities, perhaps even encompassing the present value, suffice to maintain a molten interior.

Few detailed models of Titan's internal structure have been attempted. The major stumbling blocks involve the atmosphere, whose origin and age are unclear but which must clearly have affected its thermal evolution, and the unknown behavior of ammonia monohydrate and methane clathrate at high pressures. The presence of a nitrogen-methane atmosphere implies that both kinds of ice could be present, now or in the past.

The occurrence of polymorphs of water ice (especially ices VII and VIII, which are in effect self-clathrate forms of water ice) would seem to preclude the existence of other clathrates. One might speculate that the growth of internal lithospheric pressures as Titan accreted led to the destruction of clathrates and the formation of an atmospheric coincident with accretion. But preliminary work by D. Stevenson (private communication) indicates that ammonia monohydrate may inhibit the formation of the high-pressure polymorphs of ice.

A thermal model of a Titan-sized body of ammonia hydrate, water ice, and rock in cosmic proportions was attempted by Consolmagno (1975), who concluded that large scale internal melting and differentiation would occur within 100 million years after a cold formation, and that a thin (less than 100 km) crust could be maintained to the present day. In the absence of more experimental work on the high-pressure behavior of the appropriate ices, and lacking any knowledge of the geology of Titan's surface, such models must remain quite speculative.

b. Surface Evolution

The surfaces of the Saturnian satellites are altered not only by the internal forces discussed above, but also by forces acting from outside these bodies. The most prominent of these forces is, of course, impact cratering; this topic has been examined extensively by several authors in this book and will not be discussed here. Other effects include the sublimation of ices and their destruction or alteration by solar UV radiation and high energy particles of Saturn's magnetosphere and the solar wind.

These latter effects on satellite surfaces were examined by Consolmagno and Lewis (1978). Briefly, any methane containing ice is unstable against sublimation, at Saturn's distance from the Sun; water ice, on the other hand, is clearly stable. The situation for ammonia ice is not clear cut, given the uncertainty in the vapor pressure data found by Lebofsky (1975); but, in any case, solar UV radiation is efficient enough at breaking N-H bonds (with the subsequent loss of the hot H atoms so produced) so as to eliminate ammonia from the visible top 100 μm of the surface in the space of 100 years. Thus, the observed absence of these ices in the spectra of the Saturnian satellites (Cruikshank, 1979) is not surprising.

The effect of high energy particles on the satellite surfaces has not been directly addressed, although such work is currently being undertaken for the moons of Jupiter (cf. Sieveka and Johnson, 1982). Given the lower magnetospheric fluxes around Saturn's satellites, however, it is clear that they will be less important here than near Jupiter.

An interesting comparison can be made between the reflectivity of the surfaces of the Jovian and Saturnian icy moons. Jupiter's ice-rich moons have old surfaces which are consistently darker than the younger surfaces. Almost all the icy moons of Saturn have bright surfaces, irrespective of their ages. The source of the darkening component on Ganymede and Callisto has been unclear; it may be external dust which has accumulated on their surfaces, or it may be indigenous material which was left on the surfaces while water ice was preferentially removed by sputtering and sublimation. The Saturnian and Jovian satellites have been subjected to similar fluxes of darkening material from outside these systems, but the inner satellites of Saturn have been largely isolated from the flux of impact ejecta emanating from Phoebe due to an effective sweeping up of this material by Iapetus and Titan, while the outer Galilean moons of Jupiter have experienced the full flux of impact ejecta from the irregular moons of Jupiter. Furthermore, the ejecta originating from the prograde, irregular satellites of Jupiter impact the surfaces of the larger moons of Jupiter at a much smaller velocity (approximately the escape velocity of the moons) than the ejecta from retrograde Phoebe impacts the surfaces of the Saturnian moons. Hence, the regolith of the former moons can be expected to contain a larger fraction of exogenous ejecta. We conclude that the difference in the brightness of the surfaces of the icy satellites of Jupiter and Saturn cannot be attributed to a flux of darkening material from outside these systems, but could be due to a flux of darkening material from the irregular satellites.

Alternatively, one could attribute this difference to a preferential removal of water ice from the older surfaces of the icy Jovian moons due to enhanced rates of sputtering and/or sublimation. Certainly, the Jovian moons are exposed to a higher flux of magnetospheric high energy particles and are hotter — because of their closer distance to the Sun — than are the moons of Saturn. But the older surfaces on Ganymede are brighter than similarly aged surfaces of Callisto, although Ganymede experiences a larger flux of magnetospheric particles. If sublimation is the controlling factor, it is not clear why the old surfaces of Callisto are much darker than the old surfaces of Ganymede.

In speaking of the reflectivity of the surfaces of the Saturnian moons, some comment must, of course, be made about the famous two-faced moon, Iapetus. While a number of satellites exhibit modest (approximately several tens of percent) differences in the brightness of their leading and trailing hemispheres, Iapetus is unique in having a trailing hemisphere that is about an order of magnitude brighter than its leading hemisphere (Smith et al., 1982) (fact 1). Additional constraints on the nature and source of this extreme brightness asymmetry include: At least one dark floored crater is present on the bright trailing hemisphere but no bright floored craters are obvious on the dark leading hemisphere (Smith et al., 1982) (fact 2); albedo contours in both hemispheres closely match impact flux contours (Squyres and Sagan, 1983) (fact 3); the visible and near infrared spectral reflectivity of the dark hemisphere is significantly different from that of Phoebe (Cruikshank et al., 1982) (fact 4); and the mean density of Iapetus is 1.16 ±0.09 g/cm^{-3}, indicative of an ice rich object (Smith et al., 1982). Furthermore, the discussion of Section V implied that methane, ammonia, and perhaps nitrogen and carbon monoxide may be present in these ices, besides the dominant water component (fact 5). Below, we compare the predictions of a number of theories for the brightness asymmetry with the above "facts."

Even prior to the establishment of fact 3, a number of theories were advanced in which impacting meteoroids played a prominent role in generating the brightness asymmetry. They differed in the composition of the meteoroids (icy vs carbonaceous) and in whether the key effect of the postulated impacts was erosion of native surface material or deposition of meteoroid material.

Peterson (1975) suggested that impacting icy meteoroids stuck to the trailing hemisphere of an initially dark Iapetus, but were vaporized on the leading side since their kinetic energy of impact was much greater on the leading side. This hypothesis requires an initially dark surface on Iapetus and is thus in apparent contradiction with fact 5 and the related fact that the surfaces of the inner regular satellites are bright. It is also inconsistent with fact 2.

Cook and Franklin (1970) suggested that the preferential erosion of a superficial layer of ice on the leading hemisphere exposed an underlying dark surface. This hypothesis is also inconsistent with fact 5 and, in a subtle sense, with fact 2: Most of the biggest craters on the bright side have bright interiors.

Soter (1974) proposed that dark material from Phoebe was ejected into circum-Saturnian orbits by impact events, spiralled inward under Poynting-Robertson drag, and preferentially coated the leading hemisphere of Iapetus, the first moon between Phoebe and Saturn. But in this form, Soter's hypothesis is inconsistent with fact 4.

Other hypotheses have involved purely internal origins for the dark material. For example, Smith et al. (1982) suggested that dark carbonaceous material may have been preferentially extruded on the leading hemisphere. While motivated by fact 2, such hypotheses, in their pure form, are inconsistent with fact 3.

The above discussion suggests that some type of hybrid hypothesis — involving both impacting bodies and a "native" source of the dark material — may best explain all the facts. In particular, such a hybrid hypothesis might explain both facts 2 and 3. The probable occurrence of carbon containing ices — methane and/or carbon monoxide — and the role of carbon in making dark carbonaceous chondrites and the highly absorbing aerosols in Titan's atmosphere imply that these ices are a key source for the dark material on Iapetus' surface. Squyres and Sagan (1983) proposed that this dark material contains organic chromophores produced in situ by UV irradiation of methane-containing ices. However, laboratory simulations need to be performed to determine whether such organic synthesis can occur under environmental conditions relevant for Iapetus and, if so, the efficiency of the production of compounds that strongly absorb visible radiation.

An alternative mechanism for generating dark organic material may be provided by impacting events. Gaffney and Mattson (1979) pointed out that impacts into icy satellites could provide pressures sufficient to create high density polymorphs of ice. Such impacts into a methane-clathrate surface might thus liberate methane, and possibly subject that methane to pressures and temperatures sufficient to form more complex organic materials. Such synthesis is known to occur in mixtures of gaseous methane, ammonia, and water vapor that are subjected to shock waves (Bar-Nun et al., 1970), but the nature and efficiency of the production of dark organic matter under conditions of high velocity impact into $CH_4/NH_3/H_2O$ ice mixtures are unknown.

Squyres and Sagan (1983) proposed that the albedo contrasts across Iapetus' surface arise from variations in impact flux with distance from the apex of the leading hemisphere. Variations in this flux from apex to antapex range from a factor of two for meteoroids from outside the Saturn system to almost infinity for ejecta from Phoebe. The flux variation due to a combination of both sources may be as little as a factor of two or as large as a factor of 100. According to Squyres and Sagan (1983), the net transport of material from regions of higher impact fluxes leads to a net erosion of these surfaces and hence a continual exposure of fresh methane containing ices and an easier ability of subsurface methane to diffuse to the surface. UV photolysis of the methane ice-containing surfaces results in the production of visible light absorbing organics. Conversely, surfaces of lower impact flux experience a net deposition of ejecta. Squyres and Sagan (1983) postulate that this ejecta deposit is devoid of methane ice because methane ice is readily vaporized and could thus be lost to space during repeated impact events involved in the net ballistic transport down the flux gradient. If so, regions of lower impact flux would be bright due to a nonmethane ice ejecta cover. The occurrence of a dark floored crater on the bright side could be attributed to the impact event being of recent origin. Thus, it exposed fresh methane ice and there has not been enough time yet for it to be buried by ballistic ejecta from elsewhere.

While the above hypothesis is certainly a step in the right direction, its assumptions need to be carefully scrutinized, tested, and perhaps altered. For example, might the brightness gradient be equally well produced by a combination of the generation of light absorbing chromophores by impacts rather than by UV photolysis and the net ballistic transport down the flux gradient? Do either of these mechanisms produce light absorbing chromophores in a sufficient yield? Finally, will repeated impacts lead to the volatization and loss of ices other than methane and, if so, will they perhaps cause a concentration of light absorbing chromophores in the deposited ejecta?

The central role that carbon containing ices appear to play in creating dark places on Iapetus has some interesting implications. First, the intermediate value of Hyperion's albedo might be due to a combination of processes analogous to those postulated for Iapetus and Hyperion's nonsynchronous rotation (Squyres and Sagan, 1983). Second, the high albedo of the surfaces of the satellites interior to Titan may imply that they lack carbon containing ices.

VII. Origin and Evolution of Titan's Atmosphere

There are three potential sources of Titan's atmosphere: direct retention of the gases of Saturn's primordial nebula disk by Titan's gravity ("primitive atmosphere" hypothesis), impact with volatile-rich stray bodies, especially comets ("stray body" hypothesis), and outgassing of volatiles contained in the solid material that formed the satellite ("secondary atmosphere" hypothesis). The first two of these hypotheses, with a minor exception or two, can be readily dismissed. According to solar elemental abundances (Cameron, 1973), $Ne/N \sim 1$ in the Saturn nebula. Furthermore, much of the N may have been in condensed form at the temperatures likely at Titan's distance (Pollack et al., 1976) and much of the N may have occurred as NH_3 rather than N_2 in Saturn's nebula (Prinn and Fegley, 1981). Therefore, the Ne/N_2 ratio in nebula gas captured by Titan would probably have been much greater than unity and, in any event, not less than 2. Since Ne is too heavy to readily escape from Titan's atmosphere, the mean molecular weight of its present atmosphere would be expected to be significantly less than 28, in contrast to an observed value of 28.6 (Samuelson et al., 1981). Hence, nebular gases are not a major source of Titan's atmosphere (Owen, 1982).

Because comets probably formed in very cold regions of the solar nebula, they may contain ice hydrates and clathrates. Upon impact with Titan, compounds contained in these ices could be released into the atmosphere. Because of kinetic inhibitions for the low pressures of the solar nebula, CO and N_2 are expected to be the dominant C and N containing species throughout the solar nebula (Lewis and Prinn, 1980). Thus, cometary impact with Titan would be expected to produce an atmosphere containing substantial quantities of CO and N_2. While this prediction is consistent with the occurrence of substantial amounts of N_2 in Titan's present atmosphere, it is inconsistent with CH_4 and not CO being the observed dominant C containing gas species. However, cometary impacts may be the source of the small amount of CO (~50 ppm) recently detected in Titan's atmosphere. In this case, the atmospheric CO is derived directly from CO containing ices and from chemical reactions between cometary H_2O and atmospheric CH_4 and its derivatives.

As discussed in Section V, the temperature may have been low enough in Saturn's primordial nebula disk at Titan's distance to permit the condensation of ices less volatile than water ice. Such volatiles were the major sources of Titan's atmosphere, being released when these ices were decomposed, either upon impact during accretion or in hot portions of the interior, followed by migration to the surface. Because the pressures in Saturn's nebula probably were much higher than in the solar nebula, for a fixed temperature, NH_3 and CH_4 were probably the dominant N and C containing gases in Saturn's nebula (Prinn and Fegley, 1981). For plausible nebula temperatures at Titan's distance — ~60 K (Pollack et al., 1976) — the following ices, hydrates, and clathrates may have occurred: H_2O, NH_3, $CH_4 \cdot 7\ H_2O$, $NH_3 \cdot 1\ H_2O$, $N_2 \cdot 7\ H_2O$, $CO \cdot 7\ H_2O$, $Ar \cdot 7\ H_2O$ (Lewis, 1972; Pollack et al., 1976; Owen, 1982; Strobel, 1982). As detailed below, these compounds may have served as the primary sources of atmospheric Ar, N_2, CH_4, and perhaps CO.

Ar: As discussed in Section II, Ar may be a major constituent of the atmosphere, although the evidence for its presence is indirect and subject to some uncertainty. If this inference is correct, very little could be due to ^{40}Ar resulting from the decay of ^{40}K in the interior. Using a K abundance characteristic of carbonaceous chondrites (~400 ppm) for the "rock" component of Titan and assuming complete degassing of this radiogenic Ar, we obtain a mixing ratio of only 3×10^{-4}, in contrast to a value of $\sim 10^{-1}$ obtained by Samuelson et al. (1981) for putative atmospheric Ar. Almost all of the inferred Ar would have had to have been derived from the decomposition of Ar clathrate (Owen, 1982). In this case, ^{36}Ar and ^{38}Ar would be the dominant Ar isotopes, in an approximate ratio of 5/1.

N_2: Atmospheric N_2 may have been derived, alternatively, from the decomposition of N_2 clathrate (Pollack, 1981; Owen, 1982; Strobel, 1982) or from the decomposition and volatization of NH_3 containing ices, followed by photolysis of NH_3 to N_2 (Atreya et al., 1978). Both hypotheses face potential quantitative difficulties. The amount of atmospheric N_2 derived from N_2 clathrates is limited by the following factors: NH_3 and not N_2 was probably the dominant N containing gas in Saturn's nebula; only a fraction, f, of the available nebula N_2 may have been incorporated as N_2 clathrate due to the limited amount of H_2O ice exposed to nebular gases and the formation of higher temperature clathrates from some of the exposed H_2O; and incomplete outgassing. In order for N_2 clathrates to be the dominant source of Titan's atmosphere, $f \cdot g \cdot h \cong 6 \times 10^{-3}$, where f is defined above, g is the ratio of $N_2/(NH_3 + N_2)$ in the nebula, and h is the fractional degree of outgassing. According to Prinn and Fegley (1981), $g \sim 5 \times 10^{-4}$ to 10^{-1}. Thus, N_2 clathrates are the chief source of Titan's atmospheric N_2 only if g is close to its upper bound and f and h are not much smaller than unity.

An alternative source of Titan's atmospheric N_2 is the photolysis of NH_3 vapor, resulting from the volatization of NH_3 containing ices (Atreya et al., 1978). Ammonia is irreversibly converted to N_2 by a series of photochemical reactions initiated by UV radiation at wavelengths shortward of 2300 Å. Even at Titan's distance from the Sun, there is a large enough flux of UV photons in this wavelength domain to generate several tens of bars of N_2 over the age of the solar system, provided that enough NH_3 vapor exists in Titan's atmosphere (ibid). However, temperature conditions in Titan's atmosphere may drastically diminish the production of N_2 from NH_3, perhaps to a level of insignificance: First, a negligible conversion takes place in the present day stratosphere, since the temperature minimum at the tropopause limits the NH_3 mixing ratio at higher altitudes to values $\lesssim 10^{-14}$! Second, insignificant production occurs in the troposphere due to a large attenuation of UV radiation by the highly absorbing photochemical smog layer and to the condensation of N_2H_4, an intermediate product in the photolysis cycle, at the temperatures of the troposphere.

While present day conditions in Titan's atmosphere appear to preclude significant production of N_2 from NH_3, this may not have always been the case. Of particular interest is the possibility that the atmosphere may have been much hotter during the period of Titan's formation, due to accretional heating of the surface (Lunine and Stevenson, 1982). Furthermore, the solar UV output may have been much higher at these early times (Canuto et al., 1982). But if the Saturn nebula and/or the solar nebula were present at these times, as assumed by Lunine and Stevenson (1982), grain opacity in these nebulae may have totally attenuated the solar UV radiation. In the post-accretional epoch, it may have been extremely difficult to significantly elevate the temperature at the tropopause above its present value and thus permit significant quantities of NH_3 to enter the stratosphere: The tropopause temperature is essentially a "skin" temperature, determined by the amount of sunlight Titan absorbs. Titan already has a very low albedo (~0.2; Smith et al., 1982) and the wavelength-integrated solar luminosity was probably somewhat smaller in the past (Pollack and Yung, 1980).

Nonthermal escape processes may have led to the loss of a significant fraction of Titan's N_2 to space over the age of the solar system (Strobel, 1982). Near the level of the exobase, N_2 is dissociated to N atoms at a substantial rate through impacts with energetic magnetospheric electrons. About 40% of these atoms have enough energy and are traveling in the right direction to escape from Titan's low gravitational field. Using Voyager UVS data to estimate the flux of magnetospheric electrons, Strobel (1982) estimated that Titan lost an amount of N equal to approximately 20% of the present atmospheric content due to the operation of this process over the age of the solar system. Additional loss of N to space, perhaps as much as the electron dissociation source, could have resulted from the ionization of N_2 near the exobase by magnetospheric electrons, followed by the dissociative recombination of N_2^+. Some further loss of atmospheric N_2 occurred due to the irreversible conversion of N_2 to HCN containing polymers, which sedimented out of the atmosphere (ibid).

$\underline{CH_4}$: Atmospheric methane was probably derived from the decomposition of methane clathrates. In this case, nebular temperatures below ~100 K at Titan's distance are required (Pollack et al., 1976). Absorption of solar UV radiation by methane initiates a sequence of photochemical reactions that result in a significant rate of destruction of methane. This occurs because one of the photolysis products H_2 (and its derivative H) escapes readily to space and because unsaturated hydrocarbons formed in this low H_2 mixing ratio atmosphere ultimately produce aerosols, which sediment out of the atmosphere. Photochemical calculations suggest that ~6-40 kg/cm^2 of atmospheric CH_4 has been so lost over the age of the solar system (Strobel, 1982). But the present atmosphere contains only ~0.6 kg/cm^2 of CH_4 (Samuelson et al., 1981). A comparison of these two sets of numbers implies that atmospheric CH_4 is being replenished on a quasi-continual basis, either as a result of outgassing or buffering by near-surface liquid methane.

$\underline{CO}$: As discussed earlier, plausible sources of atmospheric CO (and its derivative CO_2) include cometary CO and H_2O and volatized native CO clathrate. Because such an oxidized gas would be quickly eliminated in the reduced atmosphere of Titan, it must be quasi-continually resupplied from either or both these sources.

The occurrence of a substantial atmosphere on Titan, as contrasted to the situation for all the other satellites of the solar system, is due to the concurrent operation of the following factors (Pollack, 1981): a low enough nebular temperature to permit the occurrence of C and N containing ices (in contrast to the comparable sized Galilean satellites of Jupiter); a close enough distance to the Sun to avoid the freezing out of some major volatiles (in contrast to Triton); and a large enough mass to permit the gravitational retention of all but the lightest gases and a substantial devolatization of ices (in contrast to the other satellites of Saturn).

VIII. Origin of the Rings

Three principal theories for the origin of the rings involve formation of the present ring particle population through, alternatively, tidal disruption of a large body, condensation of material in Saturn's primordial nebula, and collisional disruption of one or several large bodies by high velocity stray bodies. The tidal disruption theory was first advanced by Roche (1847), who showed that no stable equilibrium configuration existed for a liquid satellite (i.e., one having zero tensile strength) at distances less than a critical value from its primary. This critical distance — the "Roche limit" — depends weakly on the ratio of the densities of the primary and satellite. If this ratio is not very different from unity, the Roche limit lies close to the outer boundary of the A ring. Roche proposed that a satellite evolved inward and was tidally disrupted when it crossed this limit, thereby generating Saturn's ring system. Alternatively, a stray body from outside the Saturn system could have been disrupted within the Roche limit when it passed close to Saturn.

There are, however, some very serious problems connected with a tidal origin for the rings (Pollack and Cuzzi, 1981). First, suppose that the ring material formed from a satellite of a low mass Saturn nebula or from an external object. If so, the parent body would have been a solid body, not a liquid one. Oberbeck and Aggarwal (1974) showed that the tidal disruption limit of a solid body lies much closer to the primary than that for a liquid body as a result of the finite strength of the solid body. In particular, it is not possible to tidally disrupt a solid body smaller than about 100 km at any positive altitude above Saturn's atmosphere. In the case of a larger body, the tidal limit moves out only as far as 1.4 R_s from the center of Saturn. It seems likely that if the parent body was a satellite of Saturn, it would initially have had a nearly circular orbit and its orbit would have continued to have had a low eccentricity as it evolved inward. Thus, tidal disruption of a large solid satellite would be expected to produce a ring system that was situated well inside the A and B rings, the principal rings of the Saturn system. The inner boundary of the B ring is located at 1.53 R_s.

If the parent body was a large stray body, its orbit and that of its tidally produced fragments would cross the region of the main rings. Thus, its tidal disruption could occur at closer distances without causing the problem encountered with a satellite as the parent body. However, tidal disruption can be expected to induce only very small relative velocities among the fragments. Thus, the fragments, like their parent body, would have kinetic energies in excess of the absolute values of their gravitational energies and they would escape from the Saturn system. Collisions among the fragments would cause their velocities to approach that of their parent and so not obviate the above problem.

While the above geometrical arguments offer the most severe challenge to the tidal disruption theory for solid parent bodies, it may also experience some difficulties in accounting for the size distribution of the ring particles. Harris (1975) pointed out that solid fragments of a tidally disrupted body would experience further breakup due to collisions among themselves. The kinetic energy of the colliding fragments is supplied chiefly by the gravitational potential of their partners. Greenberg et al. (1977) made several significant improvements to the calculations of Harris

(1975) and deduced that collisional evolution would result in a broad spectrum of particle sizes ranging from 1 mm to ~100 km. They suggested that the size distribution would be roughly a power law of -3.3 covering this entire range, but with most of the cross section in the centimeter-scale particles and an excess of the larger size particles, relative to the power law. Although there is evidence for the occurrence of a few "moonlets" of ~10 km size within the rings, the measured size distribution of the particles shows an abrupt change in slope from -3 for particles below ~10 m to a much steeper slope at larger sizes (Esposito et al., 1983). Such a size distribution does not appear to be in accord with the predictions of Greenberg et al. (1977).

Next, suppose that the ring material originated from condensed material in a high mass Saturn nebula. In this case, the condensates may have been composed of a liquid solution of ammonia and water, rather than solid water (cf. Fig. 7). Hence, the classical Roche theory is directly applicable: droplets forming inside the Roche limit would have been unable to gravitationally aggregate and a liquid satellite that formed outside the Roche limit and evolved through it would have been tidally disrupted. However, the total mass of the present-day rings is comparable to that of Mimas (Holberg et al., 1982). Thus, the invocation of a high mass nebula has the potential problem of requiring the elimination of almost all the condensates that formed near the region of the rings. An even more fundamental objection to this hypothesis involves the mechanism by which the satellite evolved inward to be tidally disrupted. The most obvious mechanism for radial migration is secular acceleration due to tidal interactions between the postulated satellite and Saturn. But such tidal forces cause an inward migration of the satellite only if it is situated closer to the planet than the "synchronous" distance at which an object's orbital period equals the planet's rotational period. At present, the synchronous distance is located within the Roche limit (in the outer part of the B ring). Thus, unless Saturn rotated less rapidly in its early history, any hypothetical liquid satellite forming outside the classical Roche limit would evolve outward due to tidal forces and so would not be tidally disrupted.

According to the "condensation" theory (e.g., Pollack, 1975; Pollack et al., 1977), the ring particles formed within Saturn's nebula by the same initial condensation and aggregation processes that eventually led to the formation of the regular satellites. However, only incomplete accretion occurred within the region of the rings due to tidal disruption and, hence, many small sized particles resulted rather than a single large body. The formation of water ice particles within the region of the current rings did not begin until the latter part of the satellite formation period for two reasons. First, the planet's radius extended beyond the outer boundary of the main rings at the start of stage 3. It took about 5×10^5 years of further evolution for the planet's radius to reach the inner edge of the B ring (Pollack et al., 1977). Second, the planet's luminosity had to decrease enough so that temperatures within the region of the rings fell below the condensation temperature of water vapor (~240 K). According to Figure 8, such a temperature was not reached until $\sim 5 \times 10^6$ years after the start of stage 3. If the condensation model for the rings is correct and if the nebular temperature in the region of the rings was determined primarily by Saturn's luminosity and not viscous dissipation, the above times represent a lower bound on the lifetime of Saturn's nebula. Whether the nebula could have lasted this long, in light of viscous dissipation and the accompanying inward transfer of mass, is problematical.

Once temperatures fell below the condensation point, water ice particles began to form throughout the rather extensive thickness (~10% of the radial dimension) of the nebula. Due to a combination of the vertical component of the gravitational force and gas drag, they gradually sank toward its central plane. During the settling, they continued to grow by vapor phase deposition as the nebula cooled still further and by coagulation and coalescence. Very crude calculations suggest that they could have achieved a size on the order of centimeters by the time they reached the central plane of the nebula (Pollack, 1975), in approximate accord with their observed values of 0.1 to 10^3 cm. A limited amount of further growth may have been possible as ice particles gently collided with one another and remained attached to one another by chemical "sticking" forces. However, it may have been more difficult for them to remain attached by their mutual gravity because of tidal disruption: If two particles have the same dimension, then the tidal disrupting force exceeds their mutual gravitational attraction at precisely the classical Roche limit (Pollack, 1975; Smoluchowski, 1980). But if they differ greatly in their dimensions, the tidal disruption limit lies at a much closer distance to the planet, near the inner edge of the C ring (Smoluchowski, 1980). Thus, it is not exactly clear why the ring particles have undergone as limited an amount of growth as they evidently have, although disruption by micrometeoroid impacts and other erosional agents might act to counter accretional growth.

Although moonlets having a size of ~10 km do not appear to be abundant in the rings, there is good, indirect evidence for the occurrence of at least a few moonlets of this dimension within Saturn's rings, e.g., in Encke's division in the A ring (Esposito et al., 1983). At first glance the occurrence of any such large sized objects would appear to be inconsistent with the "condensation" theory. However, it is conceivable that aggregation of centimeter to meter sized ring particles to much larger sized objects, although inhibited in most places, can occur in a few select places within the rings. For example, higher random velocities of ring particles are expected near resonance positions, such as Encke's gap. Higher velocities may promote the efficient growth of "spongy snowballs."

Because Saturn initially extended beyond the region of the rings, silicate-containing grains and/or planetesimals may have been underabundant in this region by the time it became part of the nebula: silicate-containing grains initially present there, but within Saturn's envelope, would have tended to remain with the planet. Also, silicate grains initially located at somewhat greater distances in the innermost parts of the nebula may have aggregated into planetesimals that were large enough not to be carried inward with the nebula gas as Saturn contracted. This expectation of a depletion of "rocky" material in the rings is consistent with analyses of microwave data discussed in Section II.

The condensation theory places emphasis on constructional events in the formation of the ring particles. However, they are also susceptible to disaggregation processes, particularly collisions with high velocity, stray bodies. The high crater density on the surface of Iapetus and an enhancement of the stray body flux at closer distances to Saturn due to gravitational "focusing" by Saturn imply that small satellites in the inner part of Saturn's system have a high probability of being completely fragmented over the age of the solar system (Smith et al., 1981; Shoemaker, 1982). As discussed in Section II, evidence for such catastrophic disruptions is provided by the occurrence of co-orbital satellites and the shapes of some of the satellites.

The significance of such destructive collisions for the rings is not entirely clear. Shoemaker (1982) suggests that one or several large satellites were originally present in the region of the rings and that they and their fragments suffered catastrophic collisions, resulting eventually in the present, very much smaller ring particles. This hypothesis neglects reaccretion of the fragmented material in the long intervals between destructive collisions. If tidal forces somehow prevent reaccretion, it is not clear how the original parent bodies formed in the first place. Nevertheless, collisional processes, in perhaps a much less dramatic sense than envisioned in Shoemaker's scenario, may have had an important influence on the present size distribution of ring particles.

IX. Conclusions

Here, we summarize our opinions concerning the major issues discussed in this paper and cite principal areas of uncertainty.

Formation and Evolution of Saturn

It is not yet possible to make a definitive distinction between the gas and core instability models for the origin of the giant planets in general and Saturn in particular. However, we tend to favor the core instability model for several reasons: First, it provides a natural explanation for the similar values of the core masses of all four giant planets. Second, the occurrence of irregular satellites for Jupiter and Saturn implies that accretion of asteroid-sized bodies was occurring in the outer solar system close to the time of formation of the outer planets. On aesthetic grounds, we prefer the idea of one major formation mechanism for all the bodies of the solar system, rather than two major mechanisms.

But, as detailed above, the "core" instability model has potentially very serious problems; for example, the formation times for the cores of Uranus and Neptune appear to exceed the lifetime of the solar nebula.

Numerical models, fashioned after stellar evolution models, have provided a good definition of the evolution of proto-Saturn subsequent to its formation. Major steps of evolution include an early, quasi-hydrostatic stage (stage 1), a hydrodynamical collapse stage (stage 2), and a later, quasi-hydrostatic contraction stage (stage 3). A major problem, that has hardly been addressed so far, has to do with the transfer of angular momentum between different regions of proto-Saturn from near the end of stage 1 to the beginning of stage 3. This transfer played a crucial role in the formation and nature of the Saturnian nebula within which the regular satellites formed.

Thermal cooling and contraction of a chemically homogeneous Saturn at the present epoch produce a factor of 3 less internal luminosity than is observed. The reality of this difference is strengthened by the approximate agreement of theory and observation for Jupiter. The most likely additional source of internal luminosity for Saturn is the gravitational energy released by helium sinking toward the center of Saturn in the outer part of the metallic hydrogen zone due to its partial immiscibility there. However, the thermodynamic basis for this immiscibility has been called into question.

Origin of Phoebe

Phoebe was most likely captured by gas drag when it passed through proto-Saturn just prior to the onset of stage 2. However, more refined models of the Saturn nebula at this epoch need to be developed to provide more definitive predictions of the orbital distance and object mass for which such a capture would operate. Conceivably, such models might provide a test of the two formation mechanisms, as our cursory study indicates that they may yield significantly different predictions — especially regarding the orbital distance of capture.

Origin and Evolution of the Regular Satellite System

As mentioned above, the regular satellites formed within a nebular disk that developed from proto-Saturn during the time of stage 2. In contrast to the situation for Jupiter's nebula and regular satellites, temperatures within Saturn's nebula became cool enough so that water was able to condense in all regions of satellite formation and ices containing ammonia and methane were able to form at progressively greater distances from the center of the nebula. An intriguing possibility, which is discussed at length below, is the formation of a liquid ammonia/water solution as the highest temperature condensate, rather than water ice. Such condensation may occur for the highest pressure (approximately or greater than tens of bars) and most massive (about Saturn's mass) nebular models that appear to be plausible.

The temperature of Saturn's nebula may have been controlled by Saturn's internal luminosity, which was about 5 orders of magnitude larger at the start of stage 3 than its present value. The steady decline of Saturn's internal luminosity with time led to progressively cooler nebular temperatures. Alternatively, the nebula's temperature structure may have been determined largely by internal viscous dissipation; in this case, temperatures at a given location would have also declined with time, although on a much shorter time scale. If accretion was sufficiently rapid, as perhaps suggested by recent calculations that include nebular drag, chemically zoned moons could have resulted, especially in the outer parts of the nebula.

Unfortunately, it is much more difficult to obtain estimates of Saturn's nebular density from the masses of its regular satellites than for Jupiter's nebula. A much less ordered pattern emerges (cf. Fig. 9). This difficulty might reflect the role that catastrophic collisions played in the early history of the Saturn system. All the present regular satellites, except Titan and possibly Iapetus, may be the reaccretion products of fragments of earlier, possibly larger sized moons. Clearly, a central problem of today is to further assess the role of catastrophic bombardment in shaping the Saturn system.

A minimum mass nebula is constructed by using the "systematic" nebular densities derived from the masses of Tethys, Dione, and Rhea. A maximum mass nebula is generated by assuming its mass is the same as Saturn's. Nebulae having masses toward the high mass limit have several attractive features. They allow for enough mass to produce Titan along with the other regular satellites. At the high pressures of the inner portions of these nebulae, liquid droplets of ammonia/water may condense. Satellites made in part of these droplets would start out already differentiated into rocky cores and rock-free mantles. If such satellites were broken up, the fragments would form the two populations of rocky and icy planetesimals whose random reaccretion could lead to the observed, apparently random variation in satellite densities.

One problem with massive nebulae is getting rid of the large gas mass and the extra condensed mass not currently residing in the satellites of today. In principle, most of the gas can be expected to be added to Saturn due to viscous processes within the nebula, while the remainder could be lost to space, due to angular momentum transfer. Getting rid of an amount of condensed mass in excess of that currently within the Saturn system is a more formidable problem.

In discussing the mass of Saturn's nebula, as above, it should be borne in mind that all the nebula's properties, including its mass, continually changed with time over its entire lifetime due to viscous dissipation. Thus, the above estimates are merely meant to be some crude, time-averaged values that are useful for very approximate nebular models.

Despite their comparatively small sizes, satellites such as Tethys, Dione, and Rhea experienced major tectonism (principally expansion) and resurfacing events during their first $\sim 1 \times 10^9$ years of history due to the presence of substantial quantities of ammonia in their interior makeup. Enceladus has undergone tectonism and resurfacing within the last $\sim 1 \times 10^9$ years, despite its still smaller size, probably as a result of tidal heating. If so, a significantly larger, forced orbital eccentricity than its present value appears to be required at some time in its past to initiate melting. A smaller, forced eccentricity, perhaps including the present value, suffices to maintain a molten interior.

Origin of Titan's Atmosphere

Titan's atmosphere was derived from C, N, and possibly AR containing clathrates and hydrates that helped to form the satellite. While atmospheric methane can readily be ascribed to the dissociation of methane clathrates that occurred during accretion and in the high temperature and/or high pressure environment of the satellite's interior, the source of atmospheric nitrogen is less clear. The latter gas was derived either from the direct thermal and pressure dissociation of nitrogen clathrate and/or the dissociation of ammonia hydrate, followed by UV photolysis of ammonia vapor. The first of these sources has the potential problem of being quantitatively inadequate because of the low N_2/NH_3 ratio in the Saturnian nebula, the only partial incorporation of nebular N_2 into clathrates, and the incomplete outgassing of the satellite. The second source is totally inadequate under current atmospheric conditions due to a very effective tropopause cold trap and the opacity of the aerosol layer, but it could be important for past, especially very early, atmospheres. The occurrence of a significant quantity of atmospheric Ar has not been firmly established, but, if so, this Ar was most likely derived from the dissociation of Ar clathrate. Finally, the source of the surprisingly large amount of atmospheric CO and its derivative, CO_2, remains a puzzle, although cometary and/or clathrate sources are possible.

Over the age of the solar system, large amounts of atmospheric N_2 (approximately a few tens of percent of the current abundance) and CH_4 (many times the current abundance) have been permanently eliminated from the atmosphere, through a combination of escape of selected atoms (H, N) to space and the irreversible conversion of these gases to aerosol-forming, complex organic molecules. Despite its heavy loss, atmospheric methane is maintained by the vapor pressure buffering of near-surface reservoir of methane. While this reservoir need not be in continual contact with the atmosphere, it cannot be isolated for long periods of time. Contact may occur as a result of the presence of surface oceans of methane, vapor diffusion through a regolith, or intermittent outgassing. The huge deposit of complex organic molecules residing near the surface (equivalent depth of ~0.1-1 km) represents a resource of enormous potential value to future generations.

Origin of the Rings

It seems very likely that the ring material formed within the Saturn nebula toward the end of the satellite formation period, when temperatures permitted the condensation of water in the region near the rings. An intriguing possibility, suggested by Figure 9, is that the condensate was not water ice, but a liquid water/ammonia solution. The latter forms in the high mass nebulae discussed above. If so, the classical Roche theory would be strictly applicable. In this case, the generation of a multitude of small ring particles could be attributed to the inability of liquid particles to accrete within the Roche limit or the tidal disruption of a liquid satellite, which formed outside the limit and migrated inside it. However, such a hypothesis still does not explain why satellite accretion did not occur after the particles solidified. Another open question concerns the role of early catastrophic bombardment in generating the present population of ring particles.

References

Aggarwal, H. R. and Oberbeck, V. R. (1974). Roche limit of a solid body. Astrophys. J. 191, 577-588.

Allen, M., Pinto, J. P., and Yung, Y. L. (1980). Titan: Aerosol photochemistry and variations related to the sunspot cycle. Astrophys. J. 242, L125.

Atreya, S. K., Donahue, T. M., and Kuhn, W. R. (1978). Evolution of a nitrogen atmosphere on Titan. Science 201, 611.

Bar-Nun, A., Bar-Nun, N., Bauer, S. H., and Sagan, C. (1970). Shock synthesis of amino acids in simulated primitive environments. Science 168, 470-473.

Baum, W. A., Kreidl, T., Westphal, J. A., Danielson, G. E., Seidelman, P. K., Pascu, D., and Currie, D. G. (1981). Saturn's E ring. I. CCD observations of March, 1980. Icarus 47, 84-96.

Bianchi, R., Coradini, A., Frederico, C., Lanciano, P., and Magni, G. (1982). On the formation and thermal evolution of regular satellites. In Saturn: Program and Abstracts, p. 71.

Bodenheimer, P. (1977). Calculations of the effects of angular momentum on the early evolution of Jupiter. Icarus 31, 356-368.

Bodenheimer, P., Grossman, A. S., DeCampli, W. M., Marcy, G., and Pollack, J. B. (1980). Calculations of the evolution of the giant planets. Icarus 41, 293-308.

Cameron, A. G. W. (1973). Abundances of the elements in the solar system. Space Sci. Rev. 15, 121-146.

Cameron, A. G. W. (1978). Physics of the primitive solar accretion disk. Moon and Planets 18, 5-40.

Cameron, A. G. W., DeCampli, W. M., and Bodenheimer, P. (1982). Evolution of giant gaseous protoplanets embedded in the primitive solar nebula. Icarus 49, 298-312.

Canuto, V. M., Levine, J. S., Augustsson, T. R., and Imhoff, C. L. (1982). UV radiation from the young sun and oxygen and ozone levels in the prebiological paleoatmosphere. Nature 296, 816-820.

Cheng, A. F., Lanzerotti, L. J., and Pirronello, V. (1982). Charged particle sputtering of ice surfaces in Saturn's magnetosphere. J. Geophys. Res. 87, 4567-4570.

Columbo, G. and Franklin, F. A. (1971). On the formation of the outer satellite groups of Jupiter. Icarus 15, 186-191.

Consolmagno, G. J. (1975). "Thermal history models of icy satellites." M.S. thesis, Massachusetts Institute of Technology, 202 pp.

Consolmagno, G. J. (1983a). Resurfacing Saturn's satellites: Models of partial differentiation and expansion. Submitted to Icarus.

Consolmagno, G. (1983b). Ice-rich planets and the physical properties of ice. J. Phys. Chem., in press.

Consolmagno, G. J. and Huang, P. Y. (1982). Evolution of the icy moons of Saturn. In Saturn: Program and Abstracts, p. 94.

Consolmagno, G. J. and Lewis, J. S. (1977). Preliminary thermal history models of icy satellites. In Planetary Satellites (J. Burns, ed.), Tucson: University of Arizona Press, pp. 492-500.

Consolmagno, G. J. and Lewis, J. S. (1978). The evolution of icy satellite interiors and surfaces. Icarus 34, 280-293.

Cook, A. F. and Franklin, F. A. (1970). An explanation of the light curve of Iapetus. Icarus 13, 282-291.

Coradini, A., Frederico, C., and Magni, G. (1981). Gravitational instabilities in satellite disks and formation of regular satellites. Astron. Astrophys. 99, 255-261.

Cruikshank, D. P. (1979). The surfaces and interiors of Saturn's satellites. Rev. Geophys. Space Phys. 17, 165-176.

Cruikshank, D. P., Lebofsky, L. A., Pearl, T. C., and Veverka, J. (1982). Paper presented at the International Colloquium on the Saturn System, Tucson, Ariz.

Cuzzi, J. N. and Pollack, J. B. (1978). Saturn's rings: Particle composition and size distribution as constrained by microwave observations. I. Radar observations. Icarus 33, 233-262.

Cuzzi, J. N., Pollack, J. B., and Summers, A. L. (1980). Saturn's rings: Particle composition and size distribution as constrained by observations at microwave wavelengths. II. Radar interferometric observations. Icarus 44, 683-705.

Degewij, J., Cruikshank, D. P., and Hartmann, W. K. (1980). Near-infrared calorimetry of J6 Himalia and S9 Phoebe: A summary of 0.3 to 2.2 μm reflectances. Icarus 44, 541-547.

Ellsworth, K. and Schubert, G. (1981). Thermal history models of Saturn's icy satellites. Bull. A.A.S. 13, 704.

Ellsworth, K. and Schubert, G. (1983). Saturn's icy satellites: Thermal and structural models. Submitted to Icarus.

Fink, V., Larson, H. P., Gautier, T. N., III, and Treffers, R. R. (1976). Infrared spectra of the satellites of Saturn: Identification of water ice on Iapetus, Rhea, Dione, and Tethys. Astrophys. J. Lett. 207, 63-68.

Flasar, F. M. (1973). Gravitational energy sources in Jupiter. Astrophys. J. 186, 1097-1106.

Gaffney, E. S. and Matson, D. L. (1979). High pressure phases of ice in the outer solar system. Bull. A.A.S. 11, 602.

Golitsyn, G. S. (1978). Convection in the ice crusts of satellites and its effect on surface relief. Geophys. Res. Lett. 6, 466-468.

Greenberg, R., Davis, D. R., Hartmann, W. K., and Chapman, C. R. (1977). Size distribution of particles in planetary rings. Icarus 30, 769-779.

Grossman, A. S., Pollack, J. B., Reynolds, R. T., Summers, A. L., and Graboske, H. C. (1980). The effect of dense cores on the structure and evolution of Jupiter and Saturn. Icarus 42, 358-372.

Hanel, R. et al. (1981). Infrared observations of the Saturnian system from Voyager 1. Science 212, 192-201.

Hanel, R. A., Conrath, B. J., Kunde, V. G., Pearl, J. C., and Pirraglia, T. A. (1983). Albedo, internal heat source, and energy balance of Saturn. Icarus, in press.

Harris, A. W. (1975). Collisional breakup of particles in a planetary ring. Icarus 24, 190-192.

Heppenheimer, T. A. (1975). On the presumed capture origin of Jupiter's outer satellites. Icarus 24, 172-180.

Heppenheimer, T. A. and Porco, C. (1977). New contributions to the problem of capture. Icarus 30, 385-401.

Holberg, J. B., Forrester, W. T., and Lissauer, L. T. (1982). Identification of resonance features within the rings of Saturn. Nature 297, 115-120.

Hubbard, W. B. (1980). Intrinsic luminosities of the Jovian planets. Rev. Geophys. Sp. Phys. 18, 1-9.

Hubbard, W. B. and MacFarlane, T. T. (1980). The structure of Neptune and Uranus. J. Geophys. Res. 85, 225-234.

Kieffer, H. H. (1967). Calculated physical properties of planets in relation to composition and gravitational layering. J. Geophys. Res. 72, 3179-3197.

Kuiper, G. P. (1951). On the origin of the irregular satellites. Proc. Nat. Acad. Sci. 37, 717-721.

Lange, M. A. and Ahrens, T. J. (1981). Fragmentation of ice by low velocity impact. Proc. Lunar Planet. Sci. Conf. 12B, 1667-1687.

Lebofsky, L. A. (1975). Stability of frosts in the solar system. Icarus 25, 205-217.

Lebofsky, L. A., Johnson, T. V., and McCord, T. B. (1970). Saturn's rings: Spectral reflectivity and compositional implications. Icarus 13, 226.

Lewis, J. S. (1972a). The chemistry of solar system material. Earth Planet. Sci. Lett. 15, 286.

Lewis, J. S. (1972b). Low temperature condensation from the solar nebula. Icarus 16, 241-252.

Lewis, J. S. and Prinn, R. G. (1980). Kinetic inhibition of CO and N_2 reduction in the solar nebula. Astrophys. J. 238, 357-364.

Lin, D. N. C. (1981). Convective accretion disk model for the primitive solar nebula. Astrophys. J. 246, 972-984.

Lin, D. N. C. and Papaloizou, J. (1980). On the structure and evolution of the primordial solar nebula. Mon. Not. R. Astron. Soc. 191, 37-48.

Lissauer, J. J., Shu, F. H., and Cuzzi, J. N. (1981). Moonlets in Saturn's rings? Nature 292, 707-711.

Lissauer, J. J., Peale, S. J., and Cuzzi, J. N. (1983). Ring torque on Janus and the melting of Enceladus. Submitted to Icarus.

Lunine, J. I. and Stevenson, D. J. (1982). Formation of the Galilean satellites in a gaseous nebula. Icarus 52, 14-39.

Lutz, B. L., de Bergh, C., and Owen, T. (1983). Titan: Discovery of CO in its atmosphere. Science, in press.

MacFarlane, J. L. and Hubbard, W. B. (1983). Statistical mechanics of light elements at high pressure. V. Three-dimensional Thomas-Fermi-Dirac theory. Astrophys. J., in press.

Mizuno, H. (1980). Formation of the giant planets. Progr. Theor. Phys. 64, 544-557.

Owen, T. (1982). The composition and origin of Titan's atmosphere. Planet. Space Sci. 30, 833-838.

Passey, Q. R. (1982). Viscosity of the lithosphere of Enceladus (abstract). In Saturn: Program and Abstracts, p. 73.

Peterson, C. (1975). An explanation for Iapetus' asymmetric reflectance. Icarus 24, 499-503.

Perri, F. and Cameron, A. G. W. (1974). Hydrodynamic instability of the solar nebula in the presence of a planetary core. Icarus 22, 416-425.

Pilcher, C. B., Chapman, C. R., Lebofsky, L. A., and Kieffer, H. H. (1970). Saturn's rings: Identification of water frost. Science 167, 1372.

Podolak, M. (1978). Models of Saturn's interior: Evidence for phase separation. Icarus 33, 342-348.

Pollack, J. B. (1975). The rings of Saturn. Space Sci. Rev. 18, 3-93.

Pollack, J. B. (1978). Origin and evolution of the Saturn system: Observational consequences. In The Saturn System (D. M. Hunten and D. Morrison, eds.), NASA CP-2068, pp. 9-30.

Pollack, J. B. (1981). Titan. In "The New Solar System" (J. K. Beatty, B. O'Leary, and A. Chaikin, eds.), Sky Publ. Corp., Cambridge, Mass., pp. 161-166.

Pollack, J. B. and Black, D. C. (1979). Implications of the gas compositional measurements of Pioneer Venus for the origin of planetary atmospheres. Science 205, 56-59.

Pollack, J. B. and Black, D. C. (1982). Noble gases in planetary atmospheres: Implications for the origin and evolution of planetary atmospheres. Icarus 51, 169-198.

Pollack, J. B. and Cuzzi, J. N. (1981). Rings in the solar system. Scientific American 245, 105-129.

Pollack, J. B. and Yung, Y. L. (1980). Origin and evolution of planetary atmospheres. Ann. Rev. Earth Planet. Sci. 8, 425-487.

Pollack, J. B., Summers, A., and Baldwin, B. (1973). Estimates of the size of the particles in the rings of Saturn and their cosmogonic implications. Icarus 20, 263-278.

Pollack, J. B., Grossman, A. S., Moore, R., and Graboske, H. C., Jr. (1976). The formation of Saturn's satellites and rings as influenced by Saturn's contraction history. Icarus 29, 35-48.

Pollack, J. B., Grossman, A. S., Moore, R., and Graboske, H. C. (1977). A calculation of Saturn's gravitational contraction history. Icarus 30, 111-128.

Pollack, J. B., Burns, J. A., and Tauber, M. E. (1979). Gas drag in primordial circumplanetary envelopes: A mechanism for satellite capture. Icarus 37, 587-671.

Pollack, J. B., Burns, J. A., and Moore, J. T., Jr. (1983). Properties of Saturn's F ring. In preparation.

Prentice, A. J. R. (1980). Saturn: Origin and composition of its inner moons and rings. JPL Publication 80-80.

Prentice, A. J. R. (1982). Formation of the Saturnian system: The modern Laplacian theory (abstract). In Saturn: Program and Abstracts, p. 98.

Prinn, R. G. and Fegley, B., Jr. (1981). Kinetic inhibition of CO and N_2 reduction in circumplanetary nebulae: Implications for satellite composition. Astrophys. J. 249, 308-317.

Roche, E. (1847). Acad. Sci. Letters Montpellier 243.

Safranov, V. S. (1972). Evolution of the protoplanetary cloud and formation of the Earth and planets. NASA TT F-677.

Safronov, V. S. and Ruskol, E. L. (1982). On the origin and initial temperature of Jupiter and Saturn. Icarus 49, 284-296.

Salpeter, E. E. (1973). On convection and gravitational layering in Jupiter and in stars of low mass. Astrophys. J. 181, L83-L86.

Samuelson, R. E., Hanel, R. A., Kunde, V. G., and Maguire, W. C. (1981). Mean molecular weight and hydrogen abundance of Titan's atmosphere. Nature 292, 688-693.

Samuelson, R. E., Maguire, W. C., Hanel, R. A., Kunde, V. G., Jennings, D. E., Yung, Y. L., and Aikin, A. C. (1983). CO_2 on Titan. J. Geophys. Res., in press.

See, T. J. J. (1910). Researches on the evolution of the stellar systems, Vol. II. The capture theory of cosmical evolution, Chapts. 10 and 11. R. P. Nichols and Sons, Lynn, Mass.

Shoemaker, E. (1983). Chapter in this book.

Sieveka, E. M. and Johnson, R. E. (1982). Thermal and plasma induced molecular redistribution on the icy satellites. Icarus 51, 528-548.

Slattery, W. L. (1977). The structure of the planets Jupiter and Saturn. Icarus 32, 58-72.

Slattery, W. L., DeCampli, W. M., and Cameron, A. G. W. (1980). Protoplanetary core formation by rain-out of minerals. The Moon and the Planets 23, 381-390.

Smith, B. A. et al. (1981). Encounter with Saturn: Voyager 1 imaging science results. Science 212, 163-191.

Smith, B. A. et al. (1982). A new look at the Saturn system. Science 215, 504-537.

Smoluchowski, R. (1978). Width of a planetary ring system and the C-ring of Saturn. Nature 274, 669-670.

Soter, S. (1974). Paper presented at Planetary Satellites, I.A.U. Coll. 49, Cornell University.

Squyres, S. W., Reynolds, R. T., Cassen, P. M., and Peale, S. J. (1983). The evolution of Enceladus. Icarus 53, 319-331.

Squyres, S. W. and Sagan, C. (1983). The albedo markings of Iapetus. J. Geophys. Res., in press.

Stevenson, D. J. (1980). Saturn's luminosity and magnetism. Science 208, 746-748.

Stevenson, D. J. (1982). Formation of the giant planets. Planet and Space Sci. 30, 755-764.

Stevenson, D. J. and Salpeter, E. E. (1977). The phase diagram and transport properties of hydrogen-helium fluid planets. Astrophys. J. Suppl. 35, 221-237.

Stone, E. C. and Miner, E. D. (1981). Voyager 1 encounter with the Saturnian system. Science 212, 159-162.

Strobel, D. F. (1982). Chemistry and evolution of Titan's atmosphere. Planet. Space Sci. 30, 839.

Toon, O. B., Turco, R. P., and Pollack, J. B. (1980). A physical model of Titan's clouds. Icarus 43, 260-282.

Tyler, G. L. et al. (1981). Radio science investigations of the Saturn system with Voyager 1: Preliminary results. Science 212, 201-206.

Ward, W. R. (1981). Orbital inclination of Iapetus and the rotation of the Laplacian plane. Icarus 46, 97-107.

Weidenschilling, S. J. (1978). Iron/silicate fractionation and the origin of Mercury. Icarus 35, 99-111.

Weidenschilling, S. J. (1981). Aspects of accretion in a circumplanetary nebula. Lunar Planet. Sci. XII, 1170-1172.

Weidenschilling, S. J. (1982). Origin of regular satellites. In Comparative Study of the Planets (A. Coradini and M. Fulchignoni, eds.), pp. 49-59.

Wetherill, G. W. (1981). Solar wind origin of ^{36}Ar on Venus. Icarus 46, 70-80.

Yoder, C. F. (1979). How tidal heating in Io drives the Galilean orbital resonance locks. Nature 279, 767-770.

Table 1. Observed and Inferred Properties of Saturn's Satellites
(From Smith et al., 1982 and Consolmagno, 1983b)

Name	Orbit (km)	Orbit (R_s)	Radius (km)	Mass (10^{23} g)	Density (g cm^{-3})	I/F at 0°	Central pressure (kbars)	Percent ice by mass
1980S28	137,670	2.282	10 × 20			0.4		
1980S27	139,350	2.310	70 × 50 × 40			0.6		
1980S26	141,700	2.349	55 × 45 × 35			0.6		
1980S3	151,422	2.510	70 × 60 × 50			0.4		
1980S1	151,472	2.511	110 × 100 × 80			0.4		
Mimas	185,540	3.075	196 ± 3	0.375 ±0.008[a]	1.19 ±0.05	0.7	0.1	45-60
				(0.455 ±0.054)[a]	(1.44 ±0.18)			
Enceladus	238,040	3.946	250 ±10	0.74 ±0.30	1.2 ±0.4	1.0	0.1	50-100
Tethys	294,670	4.884	530 ±10	7.55 ±0.90	1.21 ±0.16	0.8	0.6	60-90
1980S13	294,670	4.884	17 × 14 × 13			0.6		
1980S25	294,670	4.884	17 × 11 × 11			0.8		
Dione	377,420	6.256	560 ±5	10.5 ±0.3	1.43 ±0.06	0.7	0.9	50-60
1980S6	378,060	6.267	18 × 16 × 15			0.5		
Rhea	527,100	8.737	765 ±5	24.9 ±1.5	1.33 ±0.09	0.6	1.4	55-70
Titan	1,221,860	20.253	2575 ±2	1345.7 ±0.3	1.88 ±0.01	0.2	32.7	~40
Hyperion	1,481,000	24.55	205 × 130 × 110			0.2		
Iapetus	3,560,800	59.022	730 ±10	18.8 ±1.2	1.16 ±0.09	0.5	1.0	70-90
						0.05		
Phoebe	12,954,000	214.7	110 ±10			0.06		

[a]These masses are based on analyses of ground-based measurements of the positions of the Saturn moons and on using the ratio of Mimas' and Tethys' masses derived from these data and the Voyager value of Tethys' mass, respectively (see Smith et al., 1982).

Table 2. Duration of Different Stages of Accretion for Jupiter and Saturn, According to Safronon and Ruskol (1982)

Stage[a]	Duration, yr		Change in mass, units of Earth masses	
	Jupiter	Saturn	Jupiter	Saturn
1	3×10^7–1×10^8	2×10^8	1–3	2–3
2	10^5–10^6	10^6	10	8
3	2×10^2	--[b]	40	--[b]
4	10^4	6×10^4	85	20
5	10^6–10^7	10^6–10^7	120	35
6	10^8	3×10^8	60	30

[a]Stages 1, 2, 3, 4, 5, and 6 are characterized by the accretional growth of a solid core; the occurrence of an instability in the surrounding envelope, followed by a slow accretion from the surrounding solar nebula; an epoch of rapid accretion; continued accretion, but from a restricted space inside the Hill sphere; a still slower accretion limited by diffusion of the solar nebula into the now depleted feeding zone for the giant planets; and the final accretion during the dissipation of the solar nebula.

[b]Saturn does not pass through stage 3.

Table 3a. Mass Distribution in a Minimum Mass Nebula[a]

Satellite	σ obs, g cm^{-2}	σ calc, g cm^{-2}	ρ^{c}, g cm^{-3}	T, K	log P
Mimas	5,500	240,000	2.8×10^{-4}	250	0.46
Enceladus	13,000	123,000	1.2×10^{-4}	175	-0.08
Tethys	69,000	70,000	5.3×10^{-5}	125	-0.55
Dione	36,500	37,000	2.2×10^{-5}	90	-1.1
Rhea	15,000	15,000	6.6×10^{-6}	60	-1.8
Titan	86,000[b]	4,600			
Hyperion	20	2,800			
Iapetus	400	290			

[a] σ, ρ, T, and P are the nebular column mass density, volume mass density, temperature, and pressure (in bars) at the central plane, respectively.

[b] Assumes Titan's feeding zone extends to Iapetus.

[c] ρ is derived from σ : $\rho = \sigma/H$, where $H = 0.12r$ is the scale height and r is radial distance from the center of the nebula (Prinn and Fegley, 1981).

Table 3b. Maximum Mass Nebula[a]

Satellite	ρ, g cm^{-3}	T, K	log P
Mimas	8.6×10^{-2}	340	3.1
Enceladus	3.5×10^{-2}	240	2.6
Tethys	1.6×10^{-2}	175	2.1
Dione	6.7×10^{-3}	120	1.6
Rhea	2.0×10^{-3}	75	0.8

[a]Assumes $\sigma = 10^{35} r^{-2.6}$ g cm^{-2}.

Table 4. Thermal Models

Water ice and rock	Water ice, ammonium monohydrate, rock
MIMAS (present surface: old, heavily cratered, unaltered)	
Never melts, never convects; if starts molten, then refreezes by 0.1 by.	Never melts, never convects.
ENCELADUS (present surface: very young, resurfaced, relaxed craters, grooves)	
With tidal heating 5-7 times current rate, molten interior possible; crust 10-30 thick? (20X current tidal heat needed to melt from ice originally.)	With tidal heating, thinner crust likely than pure water case; needs sevenfold enhancement of current tidal heating to melt initially. The present tidal heating may suffice to keep its interior molten thereafter.
TETHYS (present surface: old, cratered; one large extensional groove)	
No interior melting, little interior convection, no significant expansion. If started molten, refreezes within 0.1 by.	33% rock, 20% NH_3H_2O. At 0.6 by, small melting at core, 1/3 km expansion; maximum melt to 130 km radius; 30 km rocky core; refreezing by 1.2 by.
DIONE (present surface: complex older cratered sections, and younger resurfaced areas; evidence for considerable expansion)	
May start with ice II core; heating changes to ice I with expansion within 0.1 by; if starts molten, refreezes by then to ice I; convection occurs, but no further melting. Later cooling may produce ice II core and contraction.	50% rock, 15% NH_3H_2O. At 0.3 by melts, contracts 0.5 km; maximum melting at 1 by to within 200 km of surface, with 150 km rocky core; expansion by 0.4 km until refrozen at 3 by; slow contraction to present.

Table 4. Concluded

Water ice and rock	Water ice, ammonium monohydrate, rock
RHEA (present surface: complex regions of differing crater histories; resurfaced plains, evidence of considerable expansion)	
Large ice II core early (unless starts molten) changing to ice I by 0.1 by; at 4.0 by, change back to ice II leads to 15 km contraction. Convection but no internal melting.	Expands 1 km until melt at 0.3 by; contracts 1.5 km until maximum melt at 1.7 by; slow 1 km expansion to present day. If ice II forms, get recent significant contraction.
TITAN (present surface: obscured by atmosphere)	
Evolution similar to Ganymede; early convection and melting possible, but likely refrozen by present.	Melts within 0.15 by; substantially differentiated by 0.5 by. Thin crust, molten convecting interior to present.
IAPETUS (present surface: light and dark hemispheres; heavily cratered)	
Smaller ice II core than Rhea; less rock so less heating and convection. No melting.	Expands by 0.8 km, melting at 0.5 by; 0.5 km contraction until refrozen at 1.2 by, with 300 km crust and 100 km rocky core. Slow half-kilometer contraction to present.

Figure Captions

Figure 1. Comparison of the sizes and densities of the satellites of Saturn (S), satellites of Jupiter (J), and other solar system objects with theoretical curves for objects made of 100% water ice (lower solid curve) and a solar elemental mixture of "rock" and "ice." From Smith et al. (1982).

Figure 2. Variation of a global (axisymmetric) instability criterion with time for different planetary formation regions. The vertical scale is the mass ratio of the protoplanet to that of the forming Sun. For values of this mass ratio above the horizontal line labeled "approximate instability threshold," the solar nebula is unstable to ring formation. After Cameron (1978).

Figure 3. Core mass as a function of total mass (core plus envelope) for conditions of hydrostatic equilibrium. The parameter f denotes the ratio of assumed grain opacity to that expected in a cold region of the solar nebula. Note that no equilibrium solutions exist for core masses exceeding certain critical values. After Mizuno (1980).

Figure 4. Evolutionary history of Saturn during the early quasi-hydrostatic and hydrodynamical collapse phases for a gas instability model. T_c, T_{eff}, R_{surf}, L, and ρ_c refer to the central temperature, effective radiating temperature, surface radius, internal luminosity, and central density, respectively. Note the scale change on the time axis between the right and left sides of the figure that correspond to the two different phases of evolution. After Bodenheimer et al. (1980).

Figure 5. Excess luminosity of Jupiter (J) and Saturn (S), in units of solar luminosity, as a function of time during the late quasi-hydrostatic stage of evolution. Observed values at the 4.5×10^9-yr time point are indicated by the square and circle for Jupiter and Saturn, respectively. Adopted from Pollack (1978).

Figure 6. Phase boundaries for the molecular and metallic phases of hydrogen and for the separation of helium from hydrogen. For points lying below the separation line, helium becomes partially immiscible in hydrogen, according to the calculations of Stevenson and Salpeter (1977). Also shown is the evolutionary track of the center and molecular/metallic boundary of a homogeneous, solar mix Saturn model of Pollack et al. (1977). Numbers next to the crosses indicate time from the start of the late, quasi-hydrostatic stage.

Figure 7. The mass distribution of the satellites of Jupiter and Saturn. To create this figure, the mass of each satellite (supplemented with sufficient gas and ice to match cosmic abundances) was spread into an annulus centered on that satellite's orbital radius and extending to the midpoints between the satellite orbits. Thus satellite mass, divided by the area of that annulus, represents the minimum surface density of material in the protoplanetary nebula. In this log-log plot, the slope of the Jovian satellites' line is -1.9 and that of the Tethys-Dione-Rhea line is -2.6, indicating that the mass distribution is controlled by a simple power law.

Figure 8. Temperature of a condensing ice grain as a function of time from the start of the late, quasi-hydrostatic stage. Each curve refers to a fixed distance from the center of the planet and is labeled by the first letter of the name of the satellite or ring segment, which is currently at that distance. The right hand, vertical scale denotes the temperature at which various ice species condense under equilibrium (E) or disequilibrium (D) conditions between the gas and solid phases. The Saturnian nebula has been assumed to be highly opaque due to grain opacity. From Pollack et al. (1976).

Figure 9. The adiabatic profiles of a minimum mass (short dashes) and maximum mass (long dashes) nebula are shown against the regions of stability of various ices in pressure-temperature space, based on the work of Lewis (1972). The minimum mass nebula has just sufficient material to make the inner regular satellites; the maximum mass nebula has one Saturn mass of material in the region of satellite formation. Note the possibility of liquid condensates in the latter case. Beyond Rhea, the nebula is likely to be isothermal since temperatures cannot drop below the ambient temperature at Saturn's distance from the Sun.

Figure 10a. The radius of Tethys (in km) as a function of time (in 10^9 years) as predicted by the thermal model of Consolmagno (1983a). The initial expansion is due to the warming of the ice; after a small degree of melting and refreezing, the planet slowly cools off and contracts.

Figure 10b. The radius of Dione (in km) as a function of time. Because Dione is denser, it presumably has more radionuclide-bearing silicates and so heats up faster than Tethys. Once it starts to melt (0.5 GYr) it contracts rapidly, then expands slowly upon refreezing until the entire body is refrozen, at 3 GYr. After that time, it slowly cools down and contracts.

Figure 10c. The radius of Rhea as a function of time. Rhea is the largest of the satellites modeled by Consolmagno (1983b) and melts the most. As with Dione, the period of melting is one when the moon contracts, and refreezing makes the moon expand again. Since refreezing may not be complete yet, it is possible that Rhea is still expanding at the present time.

Figure 10d. The radius of Iapetus as a function of time. Iapetus is large but not very dense, hence poor in radionuclides, and so it does not melt as much as Rhea. The contraction and expansion upon melting and cooling of interior sections is masked by the general cooling and contraction of the outer portions of the moon, which contain the bulk of the volume of the body.

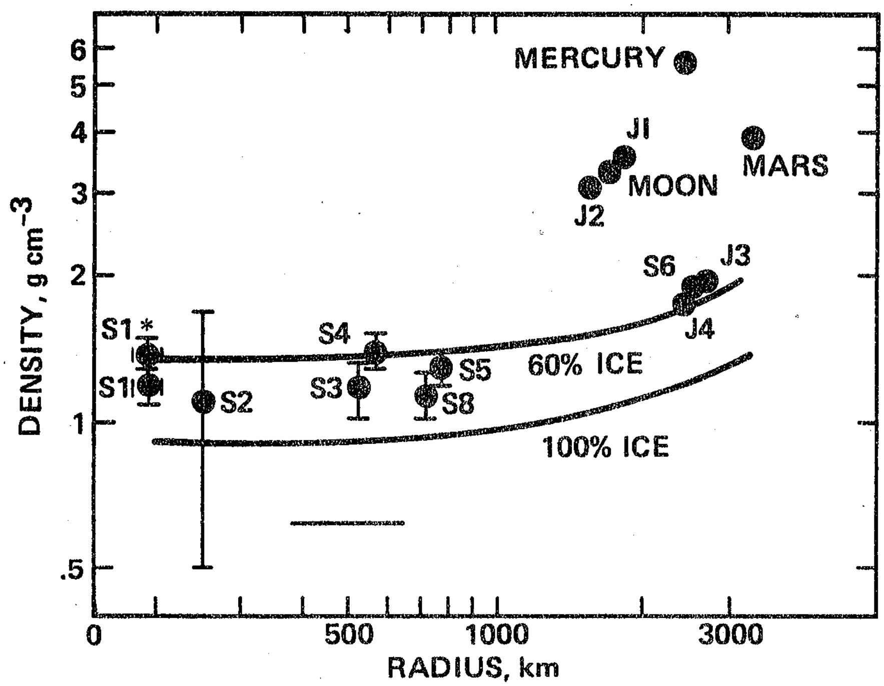
MERCURY
JI
MOON
MARS
J2
S6
J3
J4
S1*
S1I
S2
S4
S3
S5
S8
60% ICE
100% ICE
6
5
4
3
2
1
.5
DENSITY, g cm^-3
0
500
1000
3000
RADIUS, km

Fig. 1

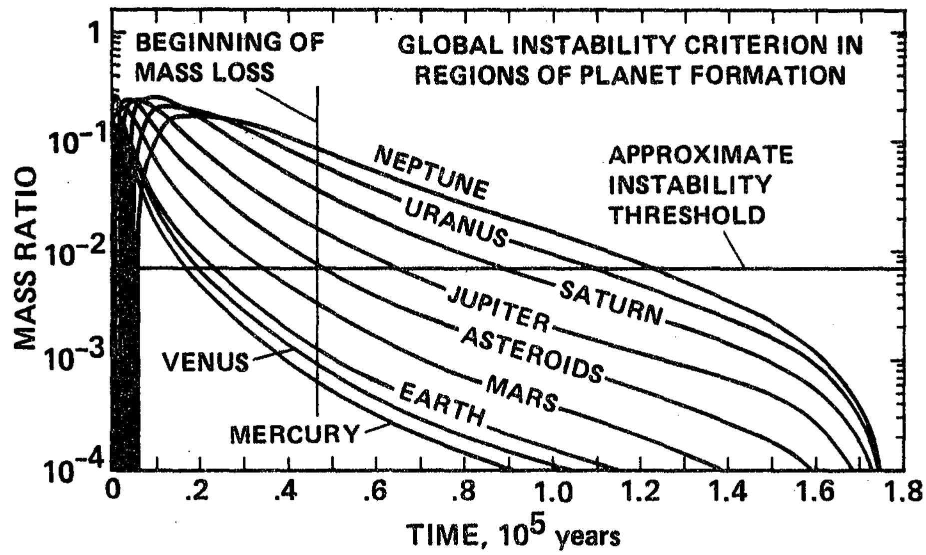

BEGINNING OF MASS LOSS
GLOBAL INSTABILITY CRITERION IN REGIONS OF PLANET FORMATION
APPROXIMATE INSTABILITY THRESHOLD
NEPTUNE
URANUS
SATURN
JUPITER
ASTEROIDS
MARS
EARTH
VENUS
MERCURY
MASS RATIO
1
10^-1
10^-2
10^-3
10^-4
0
.2
.4
.6
.8
1.0
1.2
1.4
1.6
1.8
TIME, 10^5 years

Fig. 2

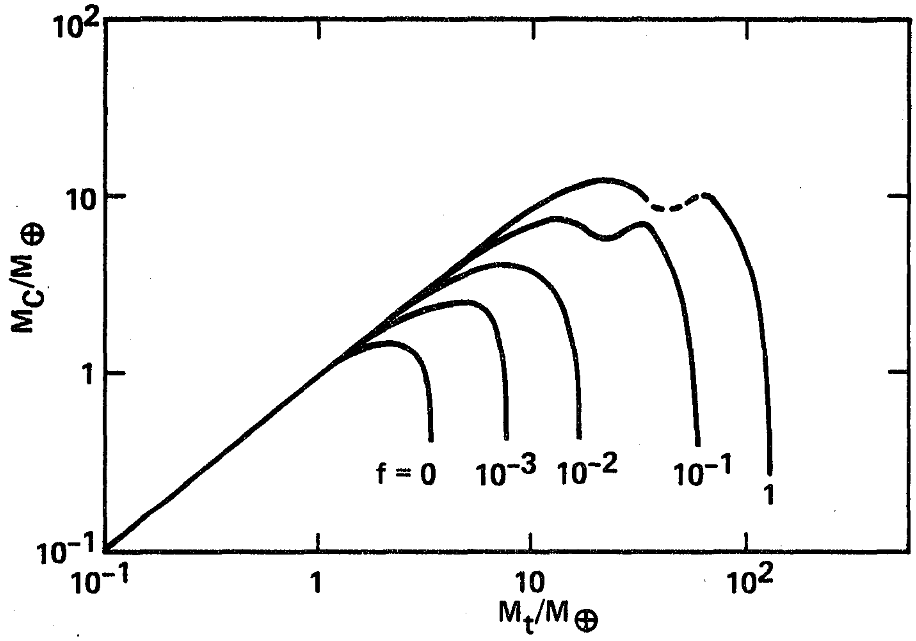

Fig. 3

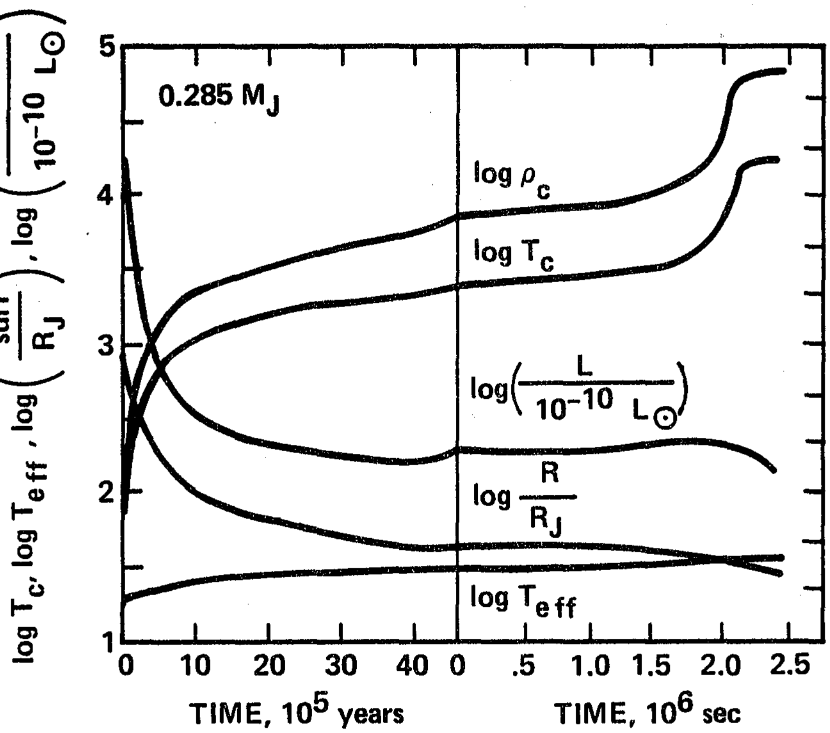
0.285 M_J
log ρ_c
log T_c
$\log\left(\frac{L}{10^{-10}\ L_\odot}\right)$
$\log \frac{R}{R_J}$
log T_{eff}
$\log T_c, \log T_{eff}, \log\left(\frac{R_{surf}}{R_J}\right), \log\left(\frac{L}{10^{-10}\ L_\odot}\right)$
TIME, 10^5 years
TIME, 10^6 sec

Fig. 4

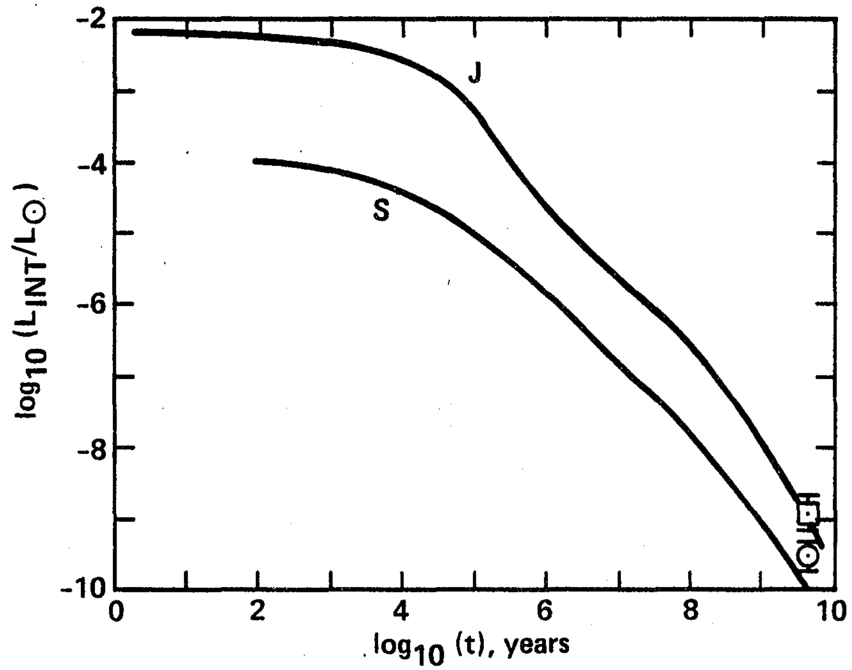

Fig. 5

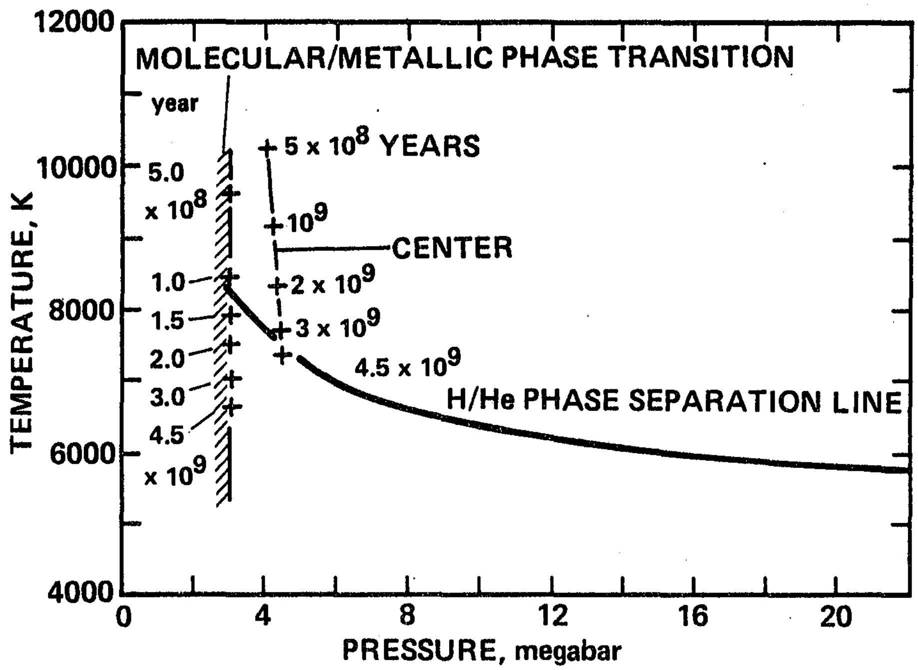

MOLECULAR/METALLIC PHASE TRANSITION
year
5.0
x 10^8
1.0
1.5
2.0
3.0
4.5
x 10^9
5 x 10^8 YEARS
10^9
CENTER
2 x 10^9
3 x 10^9
4.5 x 10^9
H/He PHASE SEPARATION LINE
12000
10000
8000
6000
4000
TEMPERATURE, K
0
4
8
12
16
20
PRESSURE, megabar

Fig. 6

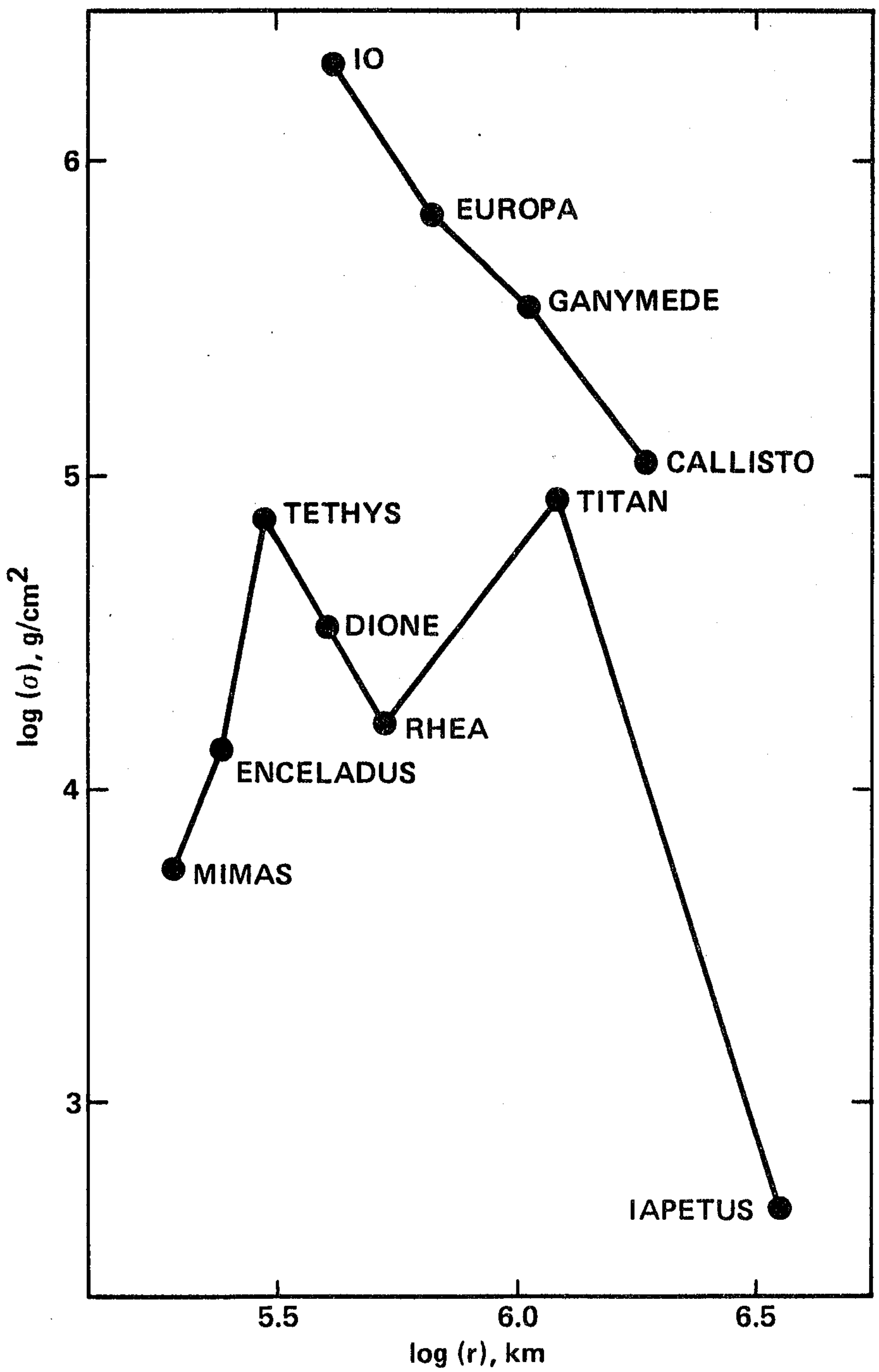
IO
EUROPA
GANYMEDE
CALLISTO
TITAN
TETHYS
DIONE
RHEA
ENCELADUS
MIMAS
IAPETUS
6
5
4
3
5.5
6.0
6.5
log (σ), g/cm²
log (r), km

Fig. 7

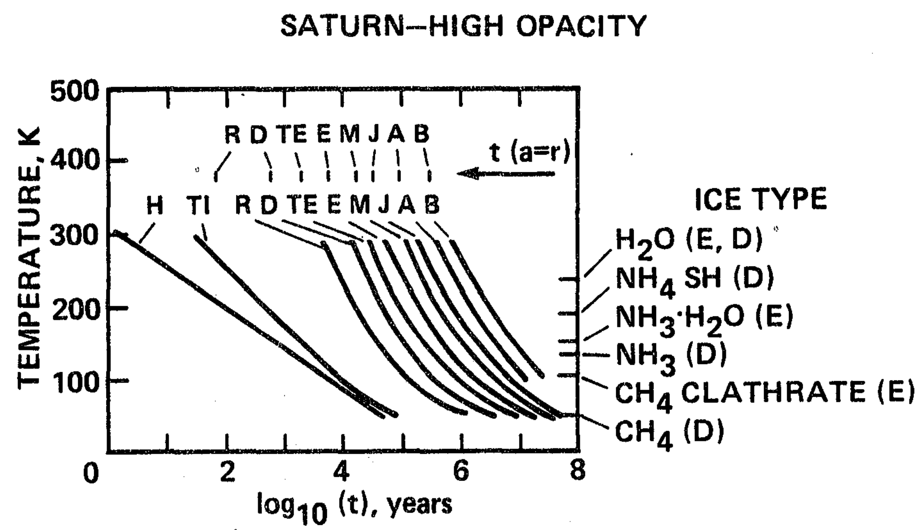
SATURN—HIGH OPACITY
TEMPERATURE, K
500
400
300
200
100
0
2
4
6
8
$\log_{10}$ (t), years
R D TE E M J A B
t (a=r)
H TI R D TE E M J A B
ICE TYPE
H_2O (E, D)
NH_4 SH (D)
$NH_3 \cdot H_2O$ (E)
NH_3 (D)
CH_4 CLATHRATE (E)
CH_4 (D)

Fig. 8

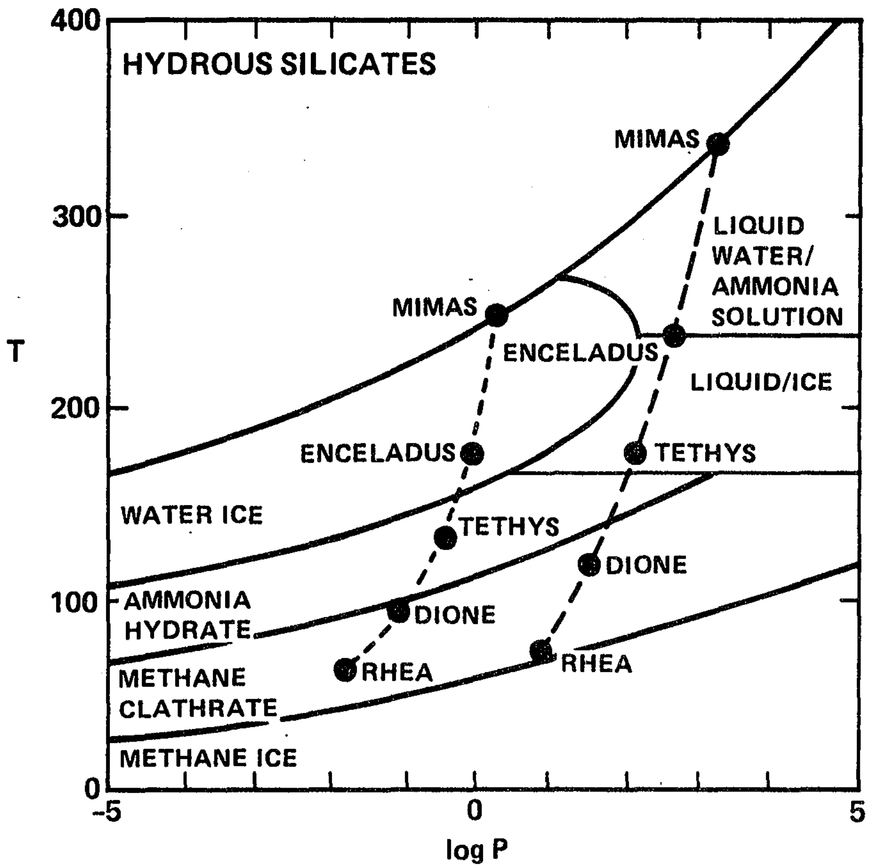
400
300
200
100
0
T
-5
0
5
log P
HYDROUS SILICATES
MIMAS
MIMAS
LIQUID
WATER/
AMMONIA
SOLUTION
ENCELADUS
LIQUID/ICE
ENCELADUS
TETHYS
WATER ICE
TETHYS
DIONE
AMMONIA
HYDRATE
DIONE
METHANE
CLATHRATE
RHEA
RHEA
METHANE ICE

Fig. 9

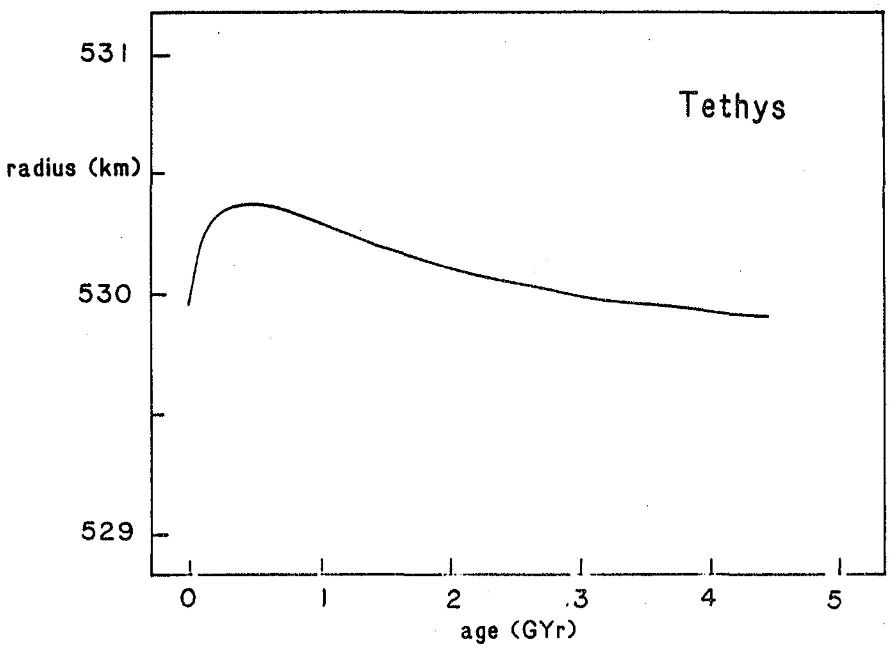

Fig. 10a

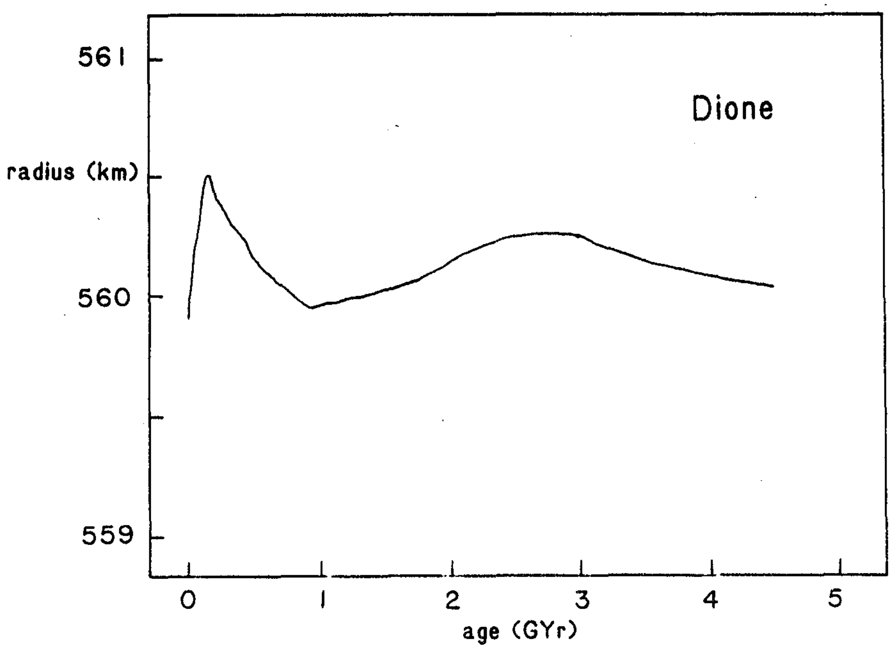

Fig. 10b

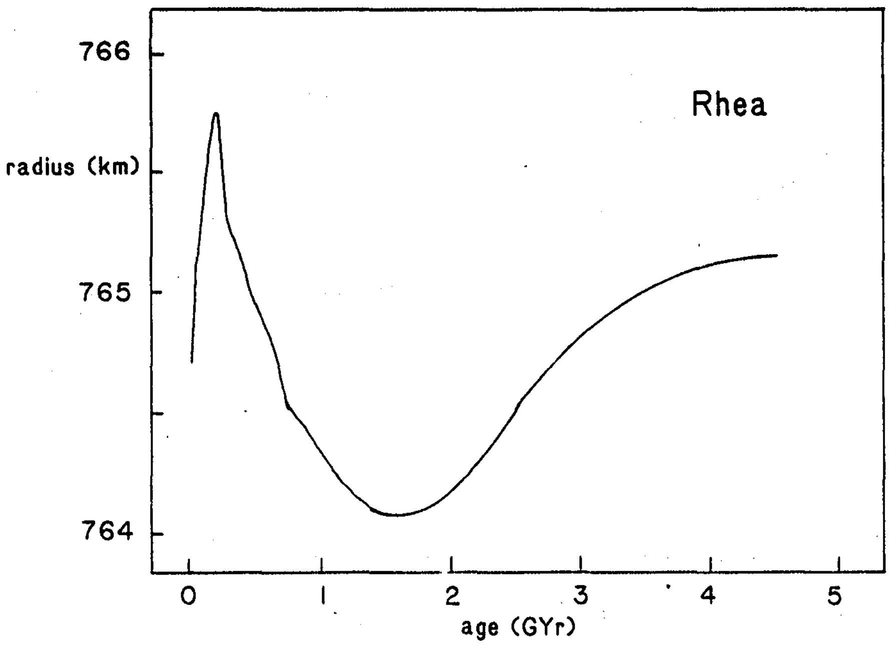

Fig. 10c

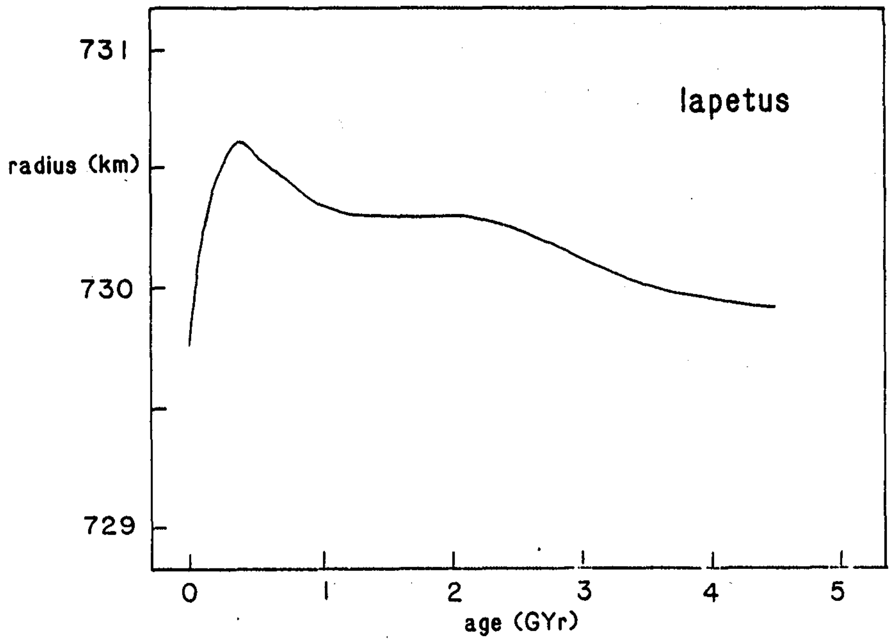

Fig. 10d

1. Report No. NASA TM-85847	2. Government Accession No.	3. Recipient's Catalog No.
4. Title and Subtitle ORIGIN AND EVOLUTION OF THE SATURN SYSTEM		5. Report Date November 1983
		6. Performing Organization Code
7. Author(s) James B. Pollack and Guy Consolmagno (Massachusetts Institute of Technology, Cambridge, Mass. 02139)		8. Performing Organization Report No. A-9485
9. Performing Organization Name and Address Ames Research Center Moffett Field, Calif. 94035		10. Work Unit No. T-5127
		11. Contract or Grant No.
12. Sponsoring Agency Name and Address National Aeronautics and Space Administration Washington, D.C. 20546		13. Type of Report and Period Covered Technical Memorandum
		14. Sponsoring Agency Code 154-10-80-18 153-03-60-01

15. Supplementary Notes

Point of contact: James B. Pollack, Ames Research Center, MS 245-3, Moffett Field, Calif. 94035 (405) 965-5530 or FTS 448-5530

To be published as a chapter in "Saturn," a book to be published by the University of Arizona.

16. Abstract

A review is provided of current concepts concerning the formation of the Saturn system and the subsequent history of the planet, its satellites, and rings. Emphasis is placed upon numerical models of Saturn's evolution and interior models of its satellites. Alternative theories are presented and assessed for the origins of the Saturn system, the rings of Saturn, and the atmosphere of Titan.

17. Key Words (Suggested by Author(s))	18. Distribution Statement
Saturn system Satellites Outer planets Rings Origin of solar system	Unlimited Subject category: 91

19. Security Classif. (of this report)	20. Security Classif. (of this page)	21. No. of Pages	22. Price*
Unclassified	Unclassified	111	A06

*For sale by the National Technical Information Service, Springfield, Virginia 22161